การประเมินปริมาณรังสีจากผลของพลังงานโฟตอนสำหรับการวางแผนการรักษาแบบสามมิติ ปรับความเข้มและปรับความเข้มแบบหมุนรอบตัวในผู้ป่วยมะเร็งปากมดลูก

นางสาววรรณิดา พูลนาผล

วิทยานิพนธ์นี้เป็นส่วนหนึ่งของการศึกษาตามหลักสูตรปริญญาวิทยาศาสตรมหาบัณฑิต
สาขาวิชาฉายาเวชศาสตร์ ภาควิชารังสีวิทยา
คณะแพทยศาสตร์ จุฬาลงกรณ์มหาวิทยาลัย
ปีการศึกษา 2560

THE DOSIMETRIC EVALUATION ON PHOTON ENERGY EFFECT FOR CERVICAL CARCINOMA IN 3D-CRT, IMRT, AND VMAT PLANS

Miss Vanida Poolnapol

A Thesis Submitted in Partial Fulfillment of the Requirements
for the Degree of Master of Science Program in Medical Imaging
Department of Radiology
Faculty of Medicine
Chulalongkorn University
Academic Year 2017

Thesis Title	THE DOSIMETRIC EVALUATION ON PHOTON ENERGY EFFECT FOR CERVICAL CARCINOMA IN 3D-CRT, IMRT, AND VMAT PLANS
By	Miss Vanida Poolnapol
Field of Study	Medical Imaging
Thesis Advisor	Taweap Sanghangthum, Ph.D.

Accepted by the Faculty of Medicine, Chulalongkorn University in Partial Fulfillment of the Requirements for the Master's Degree

.....Dean of the Faculty of Medicine

(Professor Suttipong Wacharasindhu, M.D.)

THESIS COMMITTEE

.....Chairman

(Napapat Amornwichet, M.D.,Ph.D.)

.....Thesis Advisor

(Taweap Sanghangthum, Ph.D.)

.....Examiner

(Isra Israngkul Na Ayuthaya, Ph.D.)

.....External Examiner

(Professor Franco Milano, Ph.D.)

วรรณิดา พูลนาผล : การประเมินปริมาณรังสีจากผลของพลังงานโฟตอนสำหรับการวางแผนการรักษาแบบสามมิติปรับความเข้มและปรับความเข้มแบบหมุนรอบตัวในผู้ป่วยมะเร็งปากมดลูก (THE DOSIMETRIC EVALUATION ON PHOTON ENERGY EFFECT FOR CERVICAL CARCINOMA IN 3D-CRT, IMRT, AND VMAT PLANS) อ.ที่ปรึกษาวิทยานิพนธ์หลัก: ดร. ทวีป แสงแห่งธรรม, 47 หน้า.

ในอดีตการรักษาโรคมะเร็งปากมดลูกนิยมใช้การวางแผนการรักษาแบบสามมิติ แต่ในปัจจุบันได้มีเทคโนโลยีต่างๆ ที่ช่วยพัฒนาการรักษาทางรังสีรักษาให้มีประสิทธิภาพมากยิ่งขึ้น เช่น การวางแผนการรักษาแบบปรับความเข้มและปรับความเข้มแบบหมุนรอบตัว ดังนั้นจุดประสงค์ของการศึกษานี้เพื่อเปรียบเทียบตัวแปรของปริมาณรังสีระหว่างพลังงานโฟตอน 6 และ 15 เมกะโวลต์ในแต่ละแผนการรักษาแบบสามมิติ 4 ลำรังสี แบบปรับความเข้ม 9 ลำรังสีและแบบปรับความเข้มแบบหมุนรอบตัว 2 รอบการหมุน โดยกำหนดปริมาณรังสี 50.4 เกรย์ ใน 28 ครั้งของการฉาย และใช้โปรแกรม Eclipse ในการวางแผนการรักษา ประเมินแผนการรักษาโดยใช้ตัวแปรของก้อนมะเร็ง (PTV) ได้แก่ ดัชนีบ่งบอกปริมาณรังสีที่ 95 เปอร์เซ็นต์ของปริมาตรเป้าหมาย ($D_{95\%}$) ดัชนีความครอบคลุมปริมาตรเป้าหมาย (TC) ดัชนีความสม่ำเสมอของปริมาณรังสี (HI) ดัชนีความเข้ารูป (CI) และจำนวนความเข้ารูป (CN) ตัวแปรของอวัยวะปกติ (OARs) ได้แก่ ดัชนีบ่งบอกปริมาตรเป้าหมายเมื่อได้รับปริมาณรังสี 45 และ 50 เกรย์ ($V_{45\ Gy}$ and $V_{50\ Gy}$) ปริมาณรังสีสะสมที่อวัยวะปกติ (NTID) ผลรวมของหน่วยนับวัด (MUs) เวลาขณะฉายรังสี (beam on time) และปริมาณรังสีปนเปื้อนจากนิวตรอนและแกมมา ผลการทดลองพบว่า PTV ได้รับปริมาณรังสีอย่างน้อย 50.4 เกรย์ ในขณะที่ปริมาณรังสีที่ OARs ได้ผลต่ำกว่าปริมาณรังสีที่ยอมรับได้ยกเว้นแผนการรักษาแบบสามมิติ สำหรับเทคนิคการวางแผนการรักษาแบบปรับความเข้มและปรับความเข้มแบบหมุนรอบตัวปริมาณรังสีที่ PTV และ OARs ของทั้งสองพลังงานใกล้เคียงกัน อย่างไรก็ตามค่า NTID และค่า MUs รวมถึงค่า beam on time ในแผนการรักษาโดยใช้รังสีโฟตอน 15 เมกะโวลต์ของทุกแผนการรักษาจะให้ผลลัพธ์ที่ดีกว่าแผนการรักษาที่ใช้รังสีโฟตอน 6 เมกะโวลต์ สำหรับเรื่องของรังสีปนเปื้อนขณะฉายรังสี การใช้รังสีโฟตอนพลังงาน 15 เมกะโวลต์พบว่าปริมาณนิวตรอนของแผนการรักษาแบบปรับความเข้มให้ปริมาณนิวตรอนสูงกว่าการวางแผนการรักษาแบบสามมิติและปรับความเข้มแบบหมุนรอบตัวตามลำดับเนื่องจากอิทธิพลของทิศทางของหัวเครื่องฉายรังสี ในทางตรงกันข้ามรังสีปนเปื้อนหลังฉายรังสี ณ เวลา 30 วินาที 2 นาที และ 5 นาที ได้ผลลัพธ์สัมพันธ์กับค่า MUs ทำให้การวางแผนการรักษาแบบปรับความเข้มได้ปริมาณนิวตรอนและแกมมาสูงสุด และการวางแผนการรักษาปรับความเข้มแบบหมุนรอบตัวและแบบสามมิติตามลำดับ

โดยสรุปการรักษาโรคมะเร็งปากมดลูกโดยการวางแผนการรักษาแบบสามมิติ รังสีโฟตอนพลังงานสูงให้ผลลัพธ์ที่ดีกว่าเนื่องจากปัจจัยของความเข้ารูปของเส้นแสดงปริมาณรังสี ในทางกลับกันการวางแผนการรักษาแบบปรับความเข้มการใช้พลังงาน 6 เมกะโวลต์จะให้ผลลัพธ์ที่ดีกว่าโดยเฉพาะเรื่องของรังสีปนเปื้อนจากนิวตรอนและแกมมาที่ไม่สามารถตรวจจับได้ และการวางแผนการรักษาแบบปรับความเข้มแบบหมุนรอบตัวทั้งสองพลังงานโฟตอนสามารถใช้แทนกันได้เนื่องด้วยผลลัพธ์ของทุกตัวแปรมีที่ค่าใกล้เคียงกันอย่างมีนัยสำคัญ

ภาควิชา รังสีวิทยา ลายมือชื่อนิสิต .....

สาขาวิชา ฉายาเวชศาสตร์ ลายมือชื่อ อ.ที่ปรึกษาหลัก .....

ปีการศึกษา 2560

5974043430 : MAJOR MEDICAL IMAGING

KEYWORDS: PHOTON ENERGY EFFECT / 3D-CRT / IMRT / VMAT / CERVICAL CARCINOMA

VANIDA POOLNAPOL: THE DOSIMETRIC EVALUATION ON PHOTON ENERGY EFFECT FOR CERVICAL CARCINOMA IN 3D-CRT, IMRT, AND VMAT PLANS. ADVISOR: TAWEAP SANGHANGTHUM, Ph.D., 47 pp.

In the previous time, 3D-CRT technique has been considered as the primary treatment for cervical cancer treatment. Nowadays, advanced techniques, IMRT and VMAT, are used to treat because of the dosimetric and clinical benefit over 3D-CRT technique. However, each of these technique generates difference outcomes. The purpose of this study was to investigate the dosimetric outcomes between 6 and 15 MV photon energies in each 4 fields box 3D-CRT, 9 fields IMRT, and 2 arcs VMAT plans of five advanced cervical cancers using parameters of $D_{95\%}$, TC, HI, CI, CN from PTV, $V_{45\ Gy}$ and $V_{50\ Gy}$ from OARs, NTID, MUs, beam on time, neutron dose as well as gamma dose contamination. The plans were performed on Eclipse TPS with the prescribed dose of 50.4 Gy/28F. The results showed that PTV received dose at least 50.4 Gy for all energies and techniques, while the OARs doses were lower than the tolerance limits except 3D-CRT technique. The IMRT and VMAT techniques showed the great similar PTV and OARs doses in both energy plans. The two energy IMRT and VMAT plans revealed percent volume of bladder, rectum and bowel reside in tolerance limit. However, the NTID, Mus, and beam on time in the 15 MV of all planning techniques provided better results than 6 MV plans. For radiation contamination during irradiation, the 15 MV plans presented the higher neutron dose in IMRT than 3D-CRT and VMAT, respectively due to the influence of gantry directions. While at 30s, 2mins, and 5mins after irradiation, the results were different because the outcomes relate to MUs results. Therefore, the neutron and gamma dose of VMAT were higher than 3D-CRT technique whereas IMRT delivered the highest neutron and gamma dose contamination. In conclusion, the 15 MV is recommended in 3D-CRT due to the better in CI and CN property. In contrast, the 6 MV energy is a good option for IMRT technique, since the same dosimetric parameters but 15 MV beams present neutron and gamma dose. For VMAT technique, both of photon energies are suitable to treat cervical cancer due to no significant difference in almost all outcome parameters between these two energies.

Department: Radiology Student's Signature .....

Field of Study: Medical Imaging Advisor's Signature .....

Academic Year: 2017

ACKNOWLEDGEMENTS

I would like to greatly thank Dr. Taweap Sanghangthum, Department of Radiology, Faculty of Medicine, Chulalongkorn University, my advisor for his instruct, support, care and polish my English language in this research.

I would like to greatly thank Associate Professor Sivalee Suriyapee Department of Radiology, Faculty of Medicine, Chulalongkorn University, my teacher for her instruction, support and constructive advice in the research.

I would like to deeply thank Dr. Isara Israngkul Na Ayuthaya, and all physicists at Radiotherapy Centeer, Department of Oncology, King Chulalongkorn Memmorial Hospital for a very kindness suggestion and instruction.

I would like to deeply thank Dr. Phannee saengkaew, from Department of Nuclear Engineering, Faculty of Engineering, Chulalongkorn University, for her instruct and support of neutron detectors in this research.

I would like to deeply thank Associate Professor Dr. Anchali Krisanachinda, Division of Nuclear Medicine, Department of Radiology, Faculty of Medicine, Chulalongkorn University and all lecturers and staff in the Master of Science Program in Medical Imaging, Faculty of Medicine, Chulalongkorn University for their teaching in Medical Imaging.

I would like to deeply thank to Professor Franco Milano, who is the external examiner of the thesis, for his help, kind suggestion and comments in this research.

I would like to greatly thanks to my classmate for their kind help and check grammar in my English sentence.

I would like to greatly thank all cancer patients for keeping my motivation to complete this Thesis.

Finally, I would like to greatly thank to my family for their encouragement and everything they have done to my life.

CONTENTS

Page

Page

Page

Page

LIST OF TABLES

LIST OF FIGURES

LIST OF ABBREVIATIONS

Abbreviation terms

3D-CRT	Three-dimensional conformal radiation therapy
AAA	Analytical Anisotropic Algorithm
AAPM, TG	American Association of Physicists in Medicine, Task Group
AP	Anteroposterior
B	Boron
BF_3	Boron trifluoride
BT	Brachytherapy
CI	Conformity index
cm	Centimeter
cm^3	Cubic centimeter
CN	Conformation Number
CsI (Tl)	Cesium Iodide activated by Thallium
CT	Computed tomography
CTV	Clinical target volume
cps	Count per second
$D_{2\%}$	The maximum dose to 2% of the target volume
$D_{50\%}$	The median dose to 50% of the target volume
$D_{95\%}$	The dose to 98% of the target volume
$D_{98\%}$	The minimum dose to 98% of the target volume
DVH	Dose volume histogram
EBRT	External beam radiation therapy
eV	Electronvolt
e.g.	Exempli gratia
Fx	Fractions
GTV	Gross tumour volume
Gy	Gray
HI	Homogeneity index
HPV	Human papillomavirus
hr	Hour
ICRU	International Commission on Radiation Units
IMRT	Intensity-modulated radiotherapy
ITV	Internal target volume

KCMH	King Chulalongkorn Memorial Hospital
keV	Kilo electronvolt
kg	Kilogram
LiI (Eu)	Lithium Iodide activated by Europium
LL	Left lateral
m	Meter
MeV	Mega electronvolt
mins	Minutes
MLC	Multi-leaf collimator
MRI	Magnetic resonance imaging
mSv	Millisievert
MUs	Monitor units
MV	Megavolt
n	Neutrons
NaI (Tl)	Sodium Iodide activated by Thallium
No	Number
NTID	Normal tissue to integral dose
OARs	Organs at risk
P	Phosphorus
p	Protrons
PA	Posteroanterior
PMT	Photomultiplier tubes
PTV	Planning target volume
RL	Right lateral
sec	Second
Si	Silicon
SPSS	Statistical Package for the Social Science
TC	Target coverage
TLD	Thermoluminescent dosimeter
TPS	Treatment planning system
$V_{45\ Gy}$	Volume received by 45 Gy of prescriptions dose
$V_{50\ Gy}$	Volume received by 50 Gy of prescriptions dose
VMAT	Volumetric modulated arc therapy
V_{pi}	Total volume enclosed by the prescription isodose
V_t	Target volume

$V_{t,\ pi}$	Target volume received by prescription dose or greater
Z	Atomic number
uSv	Microsievert

CHAPTER I

INTRODUCTION

1.1 Background and rationale

Cervical cancer is the fourth most common malignancy in women worldwide and it remains as a leading cause of cancer related death for women in developing countries (1). In Thai women, cervical cancer is also commonly found.

Radiotherapy is the main treatment for cervical carcinoma, separated into 2 modalities: Brachytherapy (BT) and external beam radiation therapy (EBRT). The most common treatment modality in BT for cervical cancer is called intracavitary technique that usually applies an applicator inside patient's cavity in order to transfer high dose rate radioactive to target. As a contrary, the EBRT delivers radiation dose to the target from outside patient's body and continue to the irradiation to whole pelvis. The dose of EBRT is limited by the tolerance doses to OARs such as bladder, rectum, and bowel.

Nowadays, EBRT has several techniques such as three-dimensional conformal radiation therapy (3D-CRT), intensity modulated radiation therapy (IMRT), and volumetric modulated arc therapy (VMAT). The 3D-CRT technique is the primary treatment technique for treating cervical cancer until the present time. On the other hand, the advance techniques such as IMRT and VMAT are capable to improve the efficacy for treating cervical cancer. Portlance et al. (2) showed that IMRT technique presented similar results in target coverage and more OARs sparing in comparison to 3D-CRT technique. The study from Deng X et al. (3) demonstrated significant advantages in dosimetric parameters for target and OARs in VMAT technique than the 3D-CRT technique of cervical cancer.

In addition to the treatment techniques previously described, the types of radiation and energy are also considered. Both of these factors can affect the outcomes of patient treatment since the characteristics of each radiation and energy types are different. For example, the high energy photon beams provide deeper penetration than lower energy. However, high energy beams also utilize higher MUs especially in IMRT technique. The high number of MUs can lead to neutron contamination as well as gamma contamination. Higher MUs also induces the probability of secondary malignancy in the future.

The aim of this study was to investigate the dosimetric parameters between 6 and 15 MV photon beams in 3D-CRT, IMRT, and VMAT planning techniques.

1.2 Research objective

To compare the dosimetric outcomes in advanced cervical carcinoma plans such as $D_{95\%}$, TC, HI, CI, CN from PTV, $V_{45\ Gy}$ and $V_{50\ Gy}$ from OARs, NTID, MUs, beam on time, neutron dose as well as gamma dose from contamination dose between 6 MV and 15 MV photon energies in 3D-CRT, IMRT, and VMAT plans.

CHAPTER II

REVIEW OF RELATED LITERATURES

2.1 Cervical carcinoma

2.1.1 Cervical cancer

Cervical cancer is a cancer where the abnormal cells appear in the cells lining the cervix as shown in figure 2.1. These abnormal cells have ability to invade or spread to other parts of the patient body.

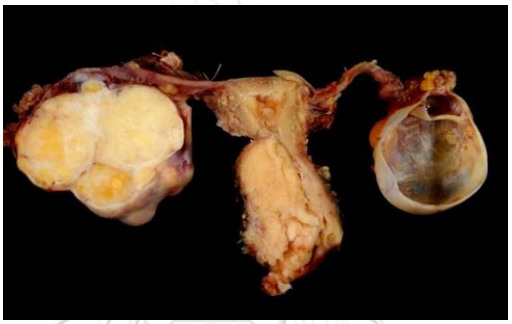

Figure 2.1 Cervical carcinoma with adnexa.

2.1.2 The incident of cervical cancer

Cervical cancer is the 4th most common cancer in women worldwide (1). In Thailand, statistics in the year 2012 showed an incidence rate of cervical cancers within 8,000 new cases. This type of cancer becomes second rank of most common cancer for Thai female (4).

2.1.3 The cause of cervical cancer (5)

The main cause of cervical cancer is Human papillomaviruses (HPV). The HPV causes the production of two proteins known as E6 and E7 which turn off some tumor suppressor genes. This may allow the cervical lining cells to grow too much and to develop changes in additional genes, which in some cases will lead to cervical cancer.

2.1.4 Treatment of choice for cervical carcinoma

The treatment options for cervical cancer are separated by staging of disease.

- **Early stage**
  - **Surgery** is the primary treatment choice to treat cervix cancer. The radical hysterectomy is one of the alternative method to treat cervical cancer. This technique removes whole uterus and lymph nodes in the pelvis and some lymph nodes from the para-aortic area.

- **Chemotherapy** is the anti-cancer drugs treatment which is injected into the bloodstream for killing the cancer cells in most parts of the body.

- Advanced stage
  - **Radiotherapy (±chemotherapy)** with both external beam radiation therapy (EBRT) and brachytherapy (BT) are the important role in radiotherapy treatment to treat cervical cancer.

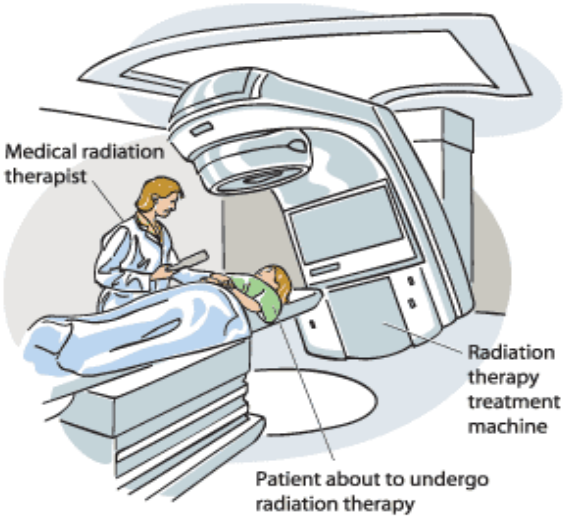

Figure 2.2 The cervical cancer external beam radiation therapy.

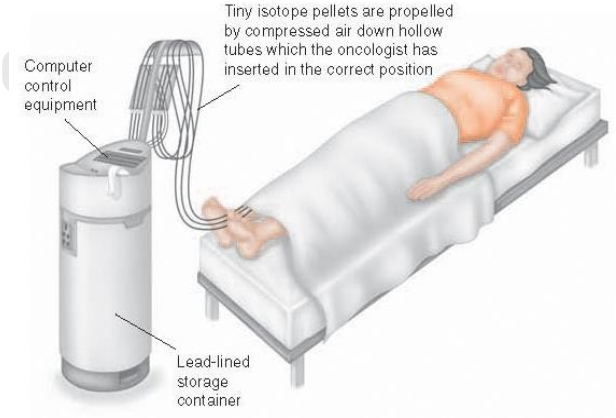

Figure 2.3 The cervical cancer intracavitary brachytherapy.

2.1.5 Radiotherapy for cervical carcinoma

- **External beam radiation therapy** as shown in figure 2.2 can be employed for 2 fields technique (AP, PA) or 4 fields technique (AP, PA, RL, LL) which is commonly known as 4 fields box technique for whole pelvis treatment. The prescription doses are conventional dose 1.8-2 Gy for 25-28 fractions with total dose of in the range of 45-50.4 Gy. There are three main critical organs which have to be concerned while treating cervical carcinoma. They are bladder, rectum, and bowel.

- **Brachytherapy** (figure 2.3) is another treatment option that delivers radiation inside the body from radioactive source. It is often used in addition to EBRT as a part of the main treatment for cervical cancer. Intracavitary technique is the most popular type of brachytherapy to treat this disease. The radioactive source placed in applicators in the vaginal canal of patient. The prescription doses are commonly in range of 6.5-8.3 Gy for 3-4 fractions according to tumor staging.

2.2 Principle of radiotherapy planning

2.2.1 Volume definition (6)

Volume of target and critical structure definition are reported by International Commission on Radiation Units (ICRU) Reports No. 50 and 62. The following volumes have been defined as principal volumes related to 3-D treatment planning (Figure 2.4), gross tumour volume (GTV), clinical target volume (CTV), internal target volume (ITV), and planning target volume (PTV).

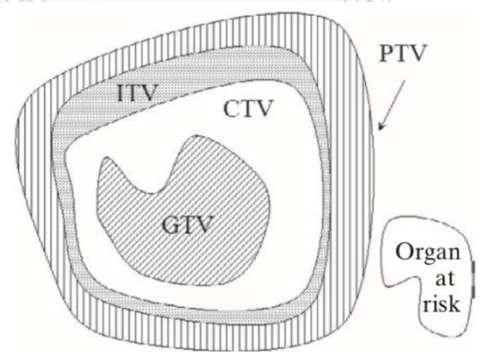

Figure 2.4 Schematic volume of target and critical structure definition reported by ICRU Reports No. 50 and 62.

2.2.1.1 Gross tumour volume (GTV)

The Gross Tumour Volume is the gross visible extent and location of malignant growth (ICRU Report No. 50). The GTV is usually based on clinical examination or on imaging modalities such as computed tomography (CT), magnetic resonance imaging (MRI), etc.

2.2.1.2 Clinical target volume (CTV)

The clinical target volume is the tissue volume that contains a demonstrable GTV and/or sub-clinical microscopic malignant disease, which has to be eliminated. This volume thus has to be treated adequately in order to achieve the aim of therapy, cure or palliation (ICRU Report No. 50).

2.2.1.3 Internal target volume (ITV)

The Internal target volume consists of the CTV plus an internal margin. The internal margin is designed to take into account the variations in the size and position of the CTV relative to the patient's reference frame. The variations due to organ motions such as breathing and bladder or rectal contents (ICRU Report No. 62).

2.2.1.4 Planning target volume (PTV)

The planning target volume is a geometrical concept, and it is defined to select appropriate beam arrangements while taking into consideration the net effect of all possible geometrical variations, in order to ensure that the prescribed dose is actually absorbed in the CTV (ICRU Report No. 50).

2.2.1.5 Organs at risk (OARs)

Organs at risk are the radiosensitive organs that can affect the total dose. The dose from a treatment plan may be significant compared with its tolerance, possibly require a change in the beam arrangement or a change in the dose. The OARs have different radiation tolerances limit based on the tissue involved.

2.2.2 Photon beam

A photon beam consists of numerous photons which pass from the target, through beam modifying devices, and into the patient or phantom. Their usefulness depends on the energy and the volume to be treated.

2.2.2.1 Photon energy

Photon energy has various types of energies such as KV X-rays, gamma rays, low and high MV X-rays. Each type of energy contains several individual characteristics such as penumbra, skin dose, and depth of maximum dose or depth of penetration. As can be seen in figure 2.5, the KV X-rays has larger penumbra than the other photon energies due to greater scatter. On the other hand, the MV X-rays have smaller penumbra because of small photon scatter and the electron range. Furthermore, the MV photon beams has more penetration property. It provides the maximum dose at Dmax as oppossed with the KV photon beams that presents the maximum dose at patient skin. Therefore, the higher energy has the skin sparing effect property better than the lower energy. Nowadays, in most of radiotherapy departments, the use of low and high energy megavoltage x-rays are commonly emplyed to treat cancer patient. The selection of

beam energy is based on the location of the tumor. For instance, in case of the tumor dwells at 12 or 15 cm depth like the prostate or cervix cancer, the suitable energy is high energy photon beams such as 10 MV beams (green line) as can be observed in figure 2.6 This is associated to the fact that 10 MV photon beams penetrates more and have better skin-sparing properties than lower energy such as 4 MV photon beams (orange line).

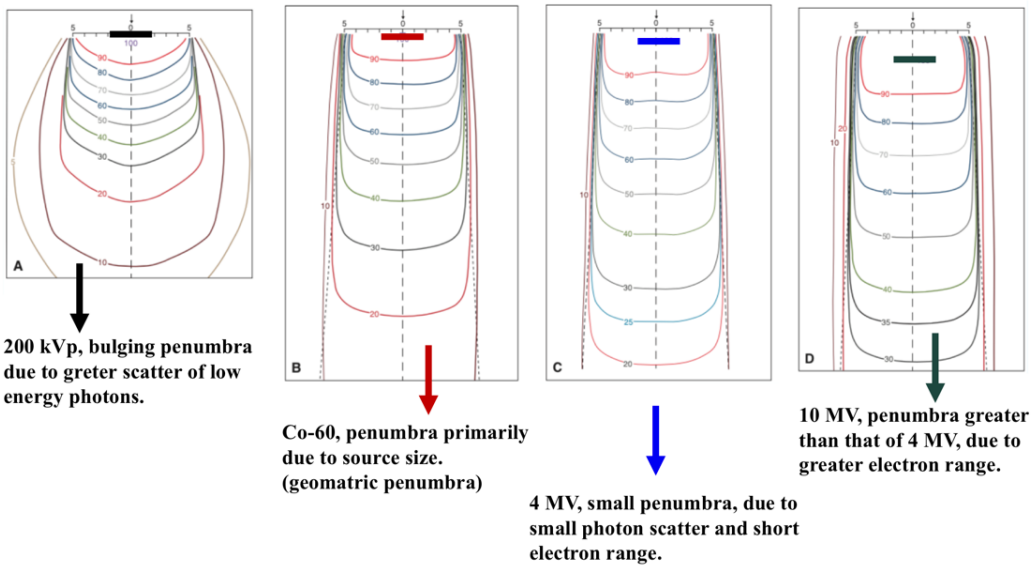

Figure 2.5 Isodose distributions for various photon beam energy.

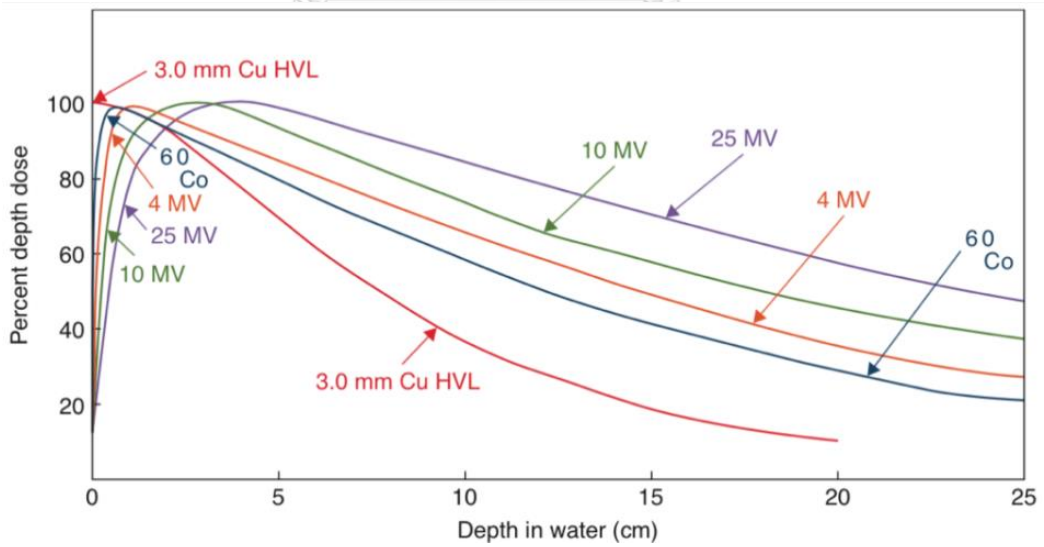

Figure 2.6 Percent depth dose for various photon beam energy.

2.2.3 External beam radiation therapy technique

One method to deliver radiation to cancer from outside patient body is the external beam radiation therapy. EBRT for cervical carcinoma is the treatment for the large field for whole pelvis including target volume and surrounding lymph node irradiation. EBRT is usually combined with BT as the boost to gross-tumor volume for cervical carcinoma treatment. ICRU Report No. 50 recommends a target dose uniformity within +7% and –5% of the prescription dose within the target. The dose of EBRT is limited by the tolerance of involved organs at risk (OARs) such as bladder, rectum, and bowel. Nowadays, EBRT has several techniques such as three-dimensional conformal radiation therapy (3D-CRT), intensity modulated radiation therapy (IMRT), and volumetric modulated arc therapy (VMAT).

2.2.3.1 3D-conformal radiation therapy (3D-CRT)

- **Overview:** 3D-CRT is the radiation therapy technique that can view a tumor in three dimensions with the help of image guidance. Therefore, this technique can deliver radiation beams from several directions to the tumor and able to conform the radiation beams to the shape of a tumor using multi-leaf collimator (MLC) for modern radiotherapy machine while limiting radiation exposure to surrounding healthy tissues. Higher beam energies (10–18 MV) are more regarded for pelvic treatments in order to increase the dose to the center and reduce dose to skin as well as subcutaneous tissues.

- **Planning technique:** 3D-CRT is the forward treatment planning where user designs the plans into a radiotherapy treatment planning system. The required decisions include beam energy, number of beams, beam directions, and prescription dose. In order to receive conformal treatment, the beam weighting, wedges, electronic tissue compensators, and other parameters need to be adjusted. The dose volume histogram (DVH) and tolerance limit of each OAR are used for planning evaluation. In cervical cancer treatment, the 4 fields box technique (figure 2.7) has been considered as the common treatment choice in 3D CRT plan.

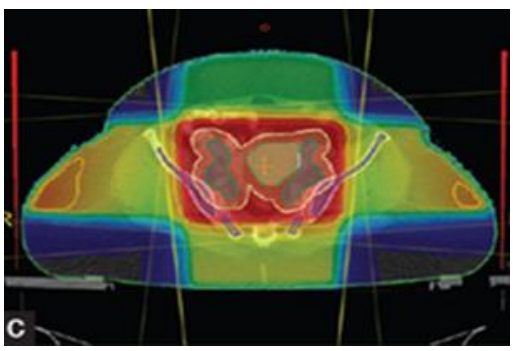

Figure 2.7 The dose distribution of 4 fields box technique in cervical cancer region.

2.2.3.2 Intensity-modulated radiotherapy (IMRT)

- **Overview:** IMRT is the technique that can create more conformal dose distribution to the target volume compared to 3D-CRT planning technique. IMRT is capable to achieve better sparing of normal surrounding tissues with the use of multiple optimized beams from different directions to create non-uniform dose distributions using MLC movement to modulate the beam (figure 2.8). However, this technique has several weaknesses. First, it gives approximately 10 times higher monitor units than 3D-CRT technique, which raises a concern about leakage radiation, secondary malignancy, and neutron contamination, especially for high energy photon beams. Second, it takes quite long time during treatment, which can increase the chances of patient movement during beam irradiation that might affect to the treatment outcome.

- **Planning technique:** IMRT is the inverse treatment planning. In contrast to the manual trial-and-error process of forward planning, the inverse planning uses the optimiser to solve the inverse problem as set by the planner. In inverse planning, radiation oncologist defines a patient's critical organs and tumour. Afterward, planner sets target doses for both tumour and organs at risk. Then, an optimization program is run to find the treatment plan which best matches to all the input criteria. Inverse planning uses the optimizer to solve the inverse problem as has been set by the planner.

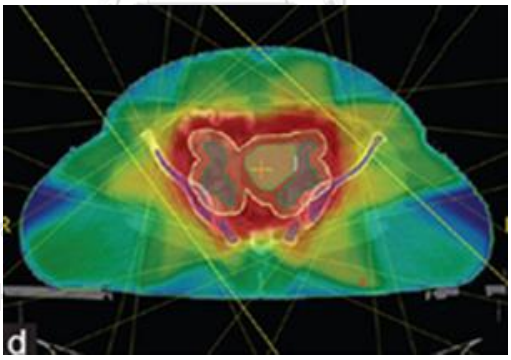

Figure 2.8 The dose distribution of 9 fields IMRT planning technique in cervical cancer region.

2.2.3.3 Volumetric modulated arc therapy (VMAT)

- **Overview:** VMAT technique is the advanced form of IMRT that can solve the disadvantage of lengthy time in IMRT planning technique. VMAT delivers a precisely sculpted 3D dose distribution during gantry rotation (figure 2.9). The machine continuously re-shapes and changes the intensity of the radiation beam as it moves around the patient with 3 modulating parameters: MLC movement, dose rate, and gantry speed variations. In addition, VMAT allows us to give lower MU in comparison to IMRT.

- **Planning technique:** VMAT is also inverse treatment planning which set up the dose constraints by the planner according to tolerance limits protocol. The result of dose distribution in VMAT planning technique is slightly similar to IMRT planning technique.

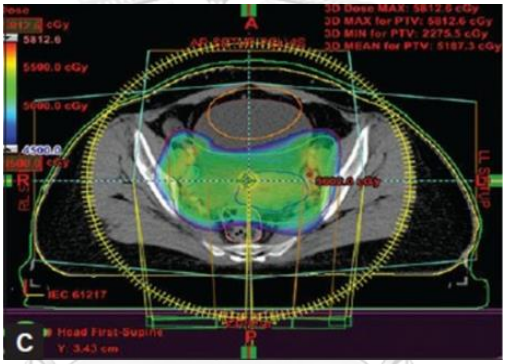

Figure 2.9 The dose distribution of 2 arcs VMAT planning technique in cervical cancer region.

2.2.4 Treatment plan evaluation (6)

After completion of plan optimization and calculation, the radiation oncologist and physicist will evaluate the plan using these following parameters: isodose curves, orthogonal planes and isodose surfaces, dose distribution statistics, and dose volume histograms.

2.2.4.1 Isodose curves and isodose surfaces

- **Isodose curves** are used to ensure that target coverage is adequate and critical structures are spared as necessary. The plan is commonly accepted within 95–100% of isodose lines, while the OARs must not exceed the tolerance limits.

- **Isodose surfaces** are the alternative way to display isodoses map in three dimensions. It shows overlay of resulting isosurface on a 3-D display featuring surface renderings of the target and/or other organs.

2.2.4.2 Orthogonal planes

Since it is impractical to evaluate the plan in only axial planes isodose distributions, the TPSs also generates the orthogonal CT planes and reconstructs the original axial data to other planes in sagittal as well as coronal isodose distributions.

2.2.4.3 Dose distribution statistics

This parameter presents the quantitative information on the volume of the target or critical structure and on the dose received by that volume. These include the minimum dose to the volume, the maximum dose to the volume, the mean dose to the volume, the dose received by at least 95% of the volume, and the volume irradiated to at least 95% of the prescribed dose.

2.2.4.4 Dose–volume histograms

A 3D treatment plan consists of dose distribution information over a 3D matrix of points over the patient's anatomy. The DVHs summarize the information contained in the 3D dose distribution and also represent a frequency distribution of dose values within PTV and contoured organs.

There are two types of DVH, these are:

- **Direct (or differential) DVHs:** The software sums the number of voxels with an average dose within a given range and plots the resulting volume. The ideal DVH for a target volume would be a single column indicating that 100% of the volume receives the prescribed dose. For a critical structure, the DVH may contain several peaks, indicating that different parts of the organ receive different doses.

- **Cumulative (or integral) DVHs:** The cumulative DVH is more popular. This parameter represents the volume of structure receiving greater than or equal to that dose. For a structure receiving a very homogenous dose (for instance, 100% of the volume receiving exactly 10 Gy), the cumulative DVH will appear as a horizontal line at the top of the graph, at 100% volume as plotted vertically with a vertical drop at 10 Gy on the horizontal axis.

2.3 Parameter Indices

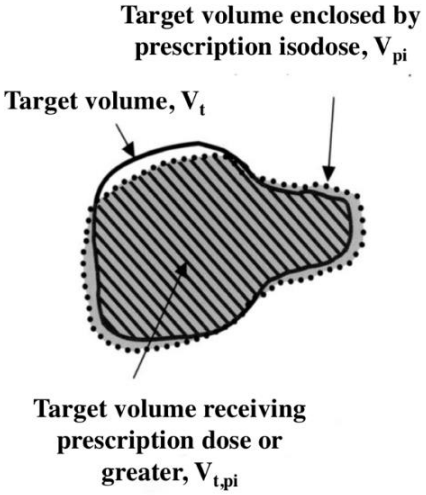

Figure 2.10 Definition of V_t, V_{pi} and $V_{t,pi}$.

2.3.1 Target coverage (TC) (7)

The target coverage is defined as the ratio of the volume of target receiving the prescription dose or greater ($V_{t,pi}$) divided by the target volume (V_t) as illustrated in figure 2.10. Equation 1 demonstrates the empirical formula to detemine the TC.

$$TC = \frac{V_{t,pi}}{V_t} \times 100\% \quad (1)$$

For perfect coverage, TC (Target coverage) = 100%. The aim of coverage is 95% and 90%-95% is acceptable for the complex treatment.

2.3.2 Conformity index (CI) (7)

The conformity index is the ratio of the volume within the target irradiated to at least the prescription isodose ($V_{t,pi}$) over the total volume enclosed by the prescription isodose (V_{pi}) from figure 2.10. Equation 2 demonstrates the empirical formula to detemine the CI.

$$CI = \frac{V_{t,pi}}{V_{pi}} \quad (2)$$

This ratio gives a value ranging from 0 (no conformity) to 1.0 (for perfect conformation, where the prescription isodose is identical to the target volume.) An ideal plan would have a CI value close to unity. The lower the ratio, the poorer the conformity.

2.3.3 Conformation number (CN) (7)

The conformation number as mathematically writte in equation 3 is the proportion of the target covered to prescription dose, which is identical to TC value in equation 1 and the volume of the tissue outside the target receiving at least the prescription dose, which is identical to CI value in equation 2.

$$CN = \frac{V_{t,pi}}{V_t} \times \frac{V_{t,pi}}{V_{pi}} \quad (3)$$

CN can have a value between 0 and 1, with 1 being the optimal conformity. The lower the score, the lesser the conformal plan is.

2.3.4 Homogeneity index (HI) (7)

The dose homogeneity index value is defined as the difference between the maximum dose delivered to 2% of the target volume ($D_{2\%}$) and the minimum dose to 98% of the target volume ($D_{98\%}$) divided by median dose ($D_{50\%}$) of the target volume as shown in equation 4.

$$HI = \frac{D_{2\%} - D_{98\%}}{D_{50\%}} \quad (4)$$

Smaller values of HI value correspond to more homogenous irradiation of the target volume. A value of 0 represents the absolute homogeneity of dose within the target.

2.3.5 Normal tissue to integral dose (NTID) (8)

To find the dose to normal tissues outside the PTV, the NTID was calculated manually and defined as a mean dose times the volume of the structure.

NTID = mean dose of (Body-PTV) (Gy) x volume of (Body-PTV) (lit) (5)

NTID has no significant impact during optimization. NTID was calculated to evaluate the quality of the plan.

2.3.6 Total number of monitor units (MUs)

The monitor unit (MUs) is a measure of machine output from a linear accelerator. Monitor units are measured by ionization chambers that measure the dose delivered by a beam and built into the treatment head of radiotherapy linear accelerators. The monitor unit is defined as monitor chamber reads 100 MU when an absorbed dose of 1 Gy is delivered to a point at the depth of maximum dose in a water-equivalent phantom whose surface is at the isocenter of the machine with a field size at the surface of 10 cm × 10 cm. (9)

2.4 Neutrons

2.4.1 Neutrons characteristics

The neutron was discovered by James Chadwick in 1932. The nature of neutrons is take place with protons within the nucleus of atom by the nuclear force as shown in figure 2.11. A neutron has mass of 1.67 x 10^{-27} kg. and also has high penetration propoty. This particles are categorized as an indirectly ionizing radiation because they do not carry an electrical charge. Ionization is caused by charged particles, which are produced during collisions with atomic nuclei. The neutrons can be classified by their energies as follows: Thermal (0.025 eV), Slow (<2 keV), Fast (> 2 keV), and Relativistic (>20 MeV). (10)

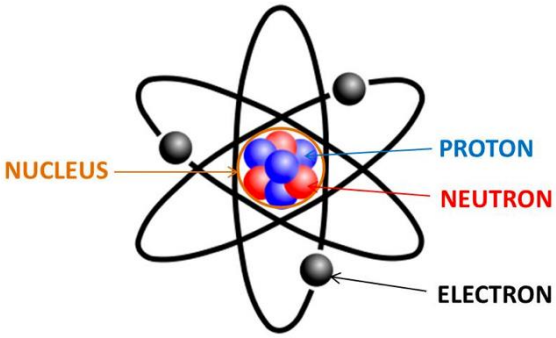

Figure 2.11 Atomic structure.

2.4.2 Photoneutron interaction

The bremsstrahlung process is confined to the target of the accelerator while the photoneutron production process (**γ**,n) occurs in both the accelerator head and treatment room. Neutron capture gamma rays are largely confined to produce in the treatment room and arises as a result from photoneutrons production when the primary photons have energies above the neutron binding energy of roughly 8 MeV for most nuclides (11). The interaction is shown in Figure 2.12.

According to AAPM TG158 (12), the photoneutron interaction is generated by interaction between photon energy which greater than 10 MV and high Z materials in the linac head such as target, primary collimators, flattening filter, upper jaw, lower jaw and multileaf collimators (MLC) (figure 2.13). The jaws or MLC can also be a major source of neutrons when they interact the primary photon beam. All neutrons are born fast then lose energy become thermal.

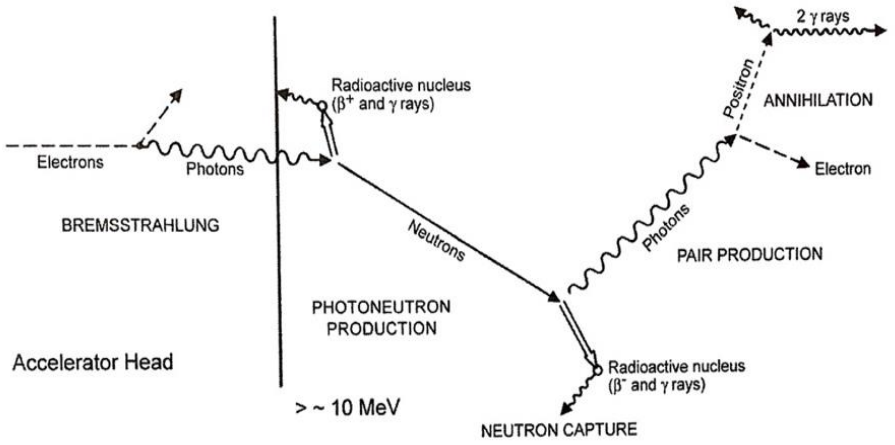

Figure 2.12 The interaction of radiation dealt with in the bremsstrahlung photons produced by linear accelerators and the secondary radiations produced by these photons.

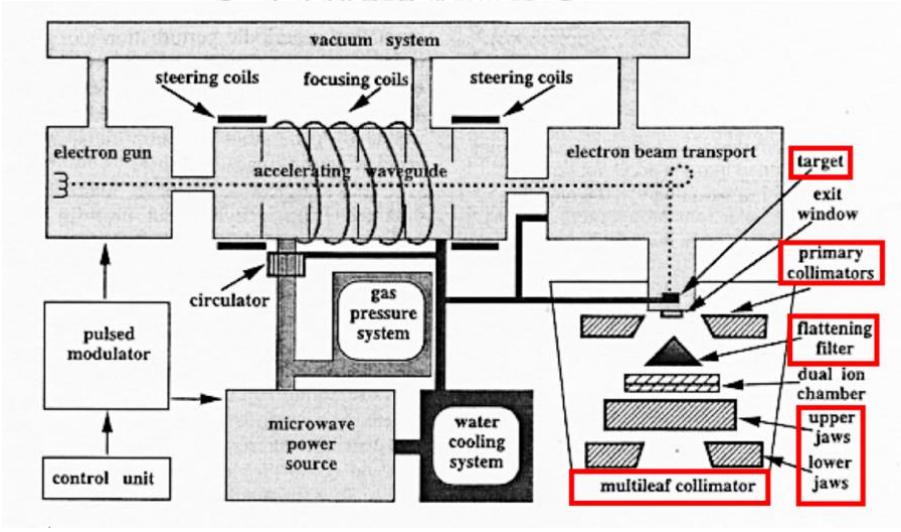

Figure 2.13 The high Z materials in the linac head.

2.4.3 Neutrons dosimetry (9)

Neutrons can be detected with the aid of their various interactions. In a hydrogenous material, neutrons produce hydrogen recoils or protons that can be detected by ionization measurements, proportional counters, and scintillation counters. Neutrons can also be detected by their nuclear reactions. Certain materials such as activation detectors could be radioactive material when exposed to neutrons. The detector, after exposure to the neutron field, is counted for beta or gamma ray activity.

Neutron measurements in or near the primary x-rays beam can be made with activation detectors, without being adversely affected by pulsed radiation. An activation detector can be used either as a bare threshold detector or inside a moderator such as polyethylene. An example of a bare threshold detector is phosphorus (in the form of phosphorus pentoxide) that has been successfully used by several investigators to measure neutrons in and outside the primary beam. A phosphorus detector can monitor both fast and thermal neutrons, using ^{31}P (n,p) ^{31} Si and ^{31}P (n, γ) ^{32}P reactions. The activation products ^{31}Si and ^{32}P are essentially pure β emitters and are counted using a calibrated liquid scintillation spectrometer.

Outside the treatment room, it is a common practice to use two detectors that respond pre-dominantly to one or the other radiation. For example, a conventional air filled ionization chamber with non-hydrogenous walls (carbon) predominantly for photon measurement and its response to neutrons can be negligible because the n:γ ratio outside the shield is usually small and the neutrons are low energy. An ion chamber with hydrogenous walls, on the other hand, can detect both neutrons and x-rays. An ion chamber that can be filled with either argon or propane to obtain a predominantly photon or photon plus neutron response, respectively, has also been used to estimate photon and neutron exposure rates outside the shield of a medical accelerator. Such a gas proportional counter, used either in the counting mode or current measurement, may be regarded as an ionization chamber with internal gas multiplication. The voltage is high enough so that ionization by collision occurs and, as a result, the current due to primary ionization is increased many fold. The basis of the detection system is the ^{10}B (n, α) ^{7}Li reaction, whereby the α particle can be counted or the ionization current caused by them is measured. A moderated BF_3 counter will also count proton recoil particles produced by neutrons in the hydrogenous material.

2.5 Detectors theory

2.5.1 Scintillation detector

Overview: The scintillation detector belongs to the class of solid state detectors. This instrument is used to detect ionizing radiation on a scintillator material and report the result in light pulses. The detector consists of scintillating phosphors (the organic and inorganic crystals contain activator atoms, emit scintillations upon absorption of radiation) and Photomultiplier tubes (PMT). The high atomic number phosphors are mostly used for the measurement of gamma rays, while the plastic scintillators are mostly used with beta particles. Example: CsI (Tl) scintillator as an example used for detection of low energy gamma waves, while LiI (Eu) Lithium iodide is used for neutron doses detection.

Operation: Start from when the radiation passes into the scintillator and interact with

atoms of crystal phosphor along the track, then produce in light photons. The number of photons is in proportion to the amount of energy of incident photons. These photons arrive to the photocathode that attached with photomultiplier tube. The photocathode emits electron for each arriving photon by the photoelectric effect. This group of primary electrons is electrostatically accelerated and focused by an electrical potential so that they strike the first dynode of the tube. The impact of a single electron on the dynode releases a number of secondary electrons which are in turn accelerated to strike the second dynode and another dynode. Each subsequent dynode impact releases further electrons, and so there is a current amplifying effect at each dynode stage. Then, these electrons pass through to the photomultiplier tubes (PMT) which converts the light to an electrical signal and electronics to process. This signal is amplified by amplifier and reported the output by monitor. The result or the number of such pulses per unit time gives information about the intensity of the radiation. The average current at the anode is used as a measure of radiation intensity as shown in figure 2.14 (13).

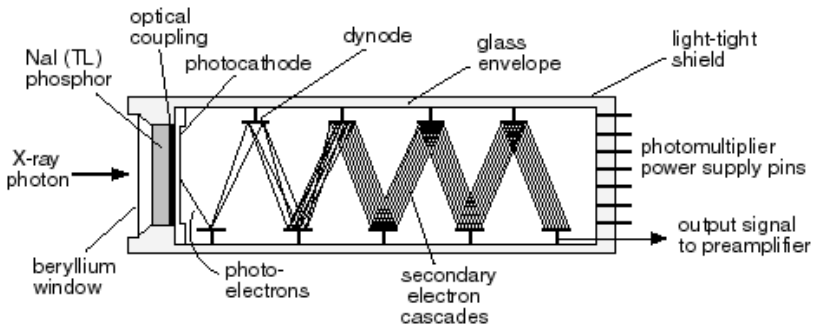

Figure 2.14 Schematic diagram of a NaI (Tl) scintillation detector.

2.5.2 Semiconductor detector

Overview: Solid-state or Semiconductor Radiation Detectors act as solid state ionization chambers on application of a reverse bias to the detectors and on exposure to radiation. The sensitivity of solid state detectors are higher than gas filled detectors, owing to the lower average energy required to produce an ion pair in solid detector materials compared with air and the higher density of the solid detector materials compared with air.

Operation: The device consists of a p-n junction across which a pulse of current develops when a particle of ionizing radiation traverses it. In a different device, the absorption of ionizing radiation generates pairs of charge carriers (electrons and holes) in a block of semiconducting material; the migration of these carriers under the influence of a voltage maintained between the opposite faces of the block constitutes a pulse of current. The pulses created in this way are amplified, recorded, and analyzed to determine the energy, number, or identity of the incident-charged particles. The diagram of solid-state detector is shown in figure 2.15 (14).

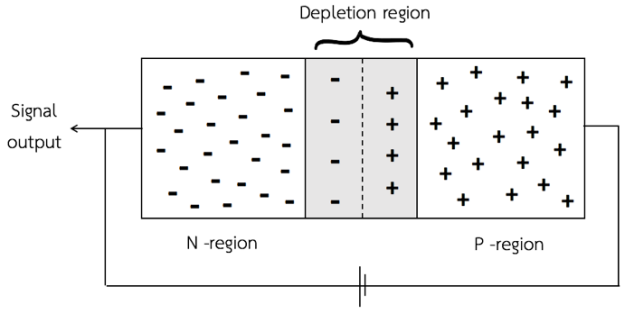

Figure 2.15 Schematic of a solid state detector.

2.6 Review of related literatures

The first literature review, J. Forrest et al. (15) studied in a dosimetric planning study comparing Intensity-modulated Radiotherapy with four-field conformal pelvic radiotherapy for the definitive treatment of cervical carcinoma. This study aimed to compare the dose to organs at risk between a conventional four-field whole pelvis radiotherapy (4F-WPRT) plan and an initial single intensity-modulated WPRT (IM-WPRT) plan for a definitive treatment of cervical cancer. They found that the target coverage at 95% of PTV was not much different between 2 plans and the percent mean dose of OARs reduced when using IMRT technique. In conclusion, their study found that an initial single IMRT plan can produce the significant of dose sparing to OAR in all organs in nearly all patients, while maintaining target coverage.

The second literature review, A dosimetric analysis of 6 MV versus 15 MV photon energy plans for intensity modulated radiation therapy (IMRT) of carcinoma of cervix was performed by A. Tyagi et al. (8). This research aimed to compare the dosimetric parameters in IMRT plans generated by 6MV and 15MV photon energies for cervical cancer. Their result showed a comparable coverage of planning target volume (PTV) and organ at risk (OAR) for both energies. The parameter indices of homogeneity index (HI) and conformity index at 98% ($CI_{98\%}$) for both energies were similar while integral dose to normal tissue (NTID) and total number of monitor units (MUs) were lesser in 15 MV plans compared to 6MV plans. Therefore, they concluded that a 6 MV IMRT photon was a good choice for cervix carcinoma as it generated a highly conformal and homogeneous plan with the good target coverage and OARs sparing.

The third literature review, F. Vanhavere et al. (16) illustrated neutron and gamma peripheral doses around a medical accelerator in 6 and 18 MV photon energies of IMRT techniques by using TLD for prostate cancer. They found the doses in free air were higher for 18 MV compared with 6 MV beam. For the 6 MV at 1 m. to isocenter beam, the neutron and gamma dose could be neglected, while the neutron and gamma dose were higher for the 18 MV at 1 m. to isocenter because of the higher number of monitor units.

CHAPTER III

RESEARCH METHODOLOGY

3.1 Research design

This study is an observational analytical study.

3.2 Research design model

The diagram of research design model is shown in figure 3.1 and figure 3.2 for part 1 and part 2, respectively.

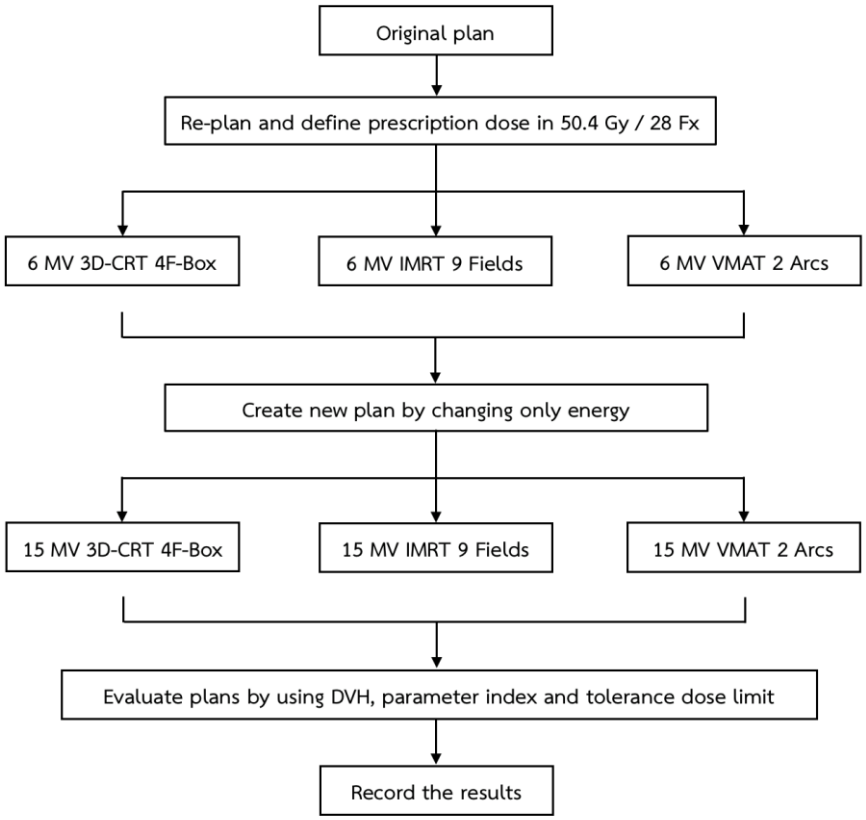

Figure 3.1 Research design model part 1.

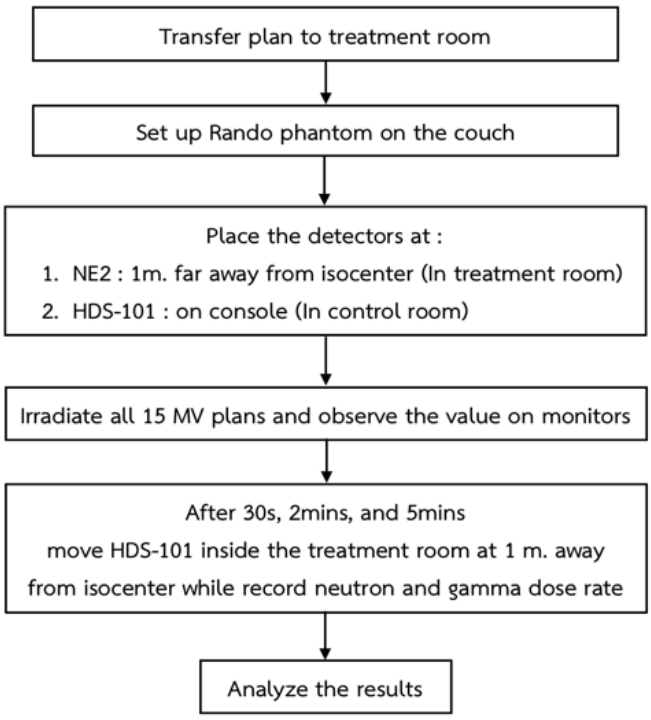

Figure 3.2 Research design model part 2.

3.3 Conceptual framework

The factors that affect to the dosimetric outcomes are photon energies, treatment techniques and parameter indices. The diagram of conceptual framework is shown in figure 3.3.

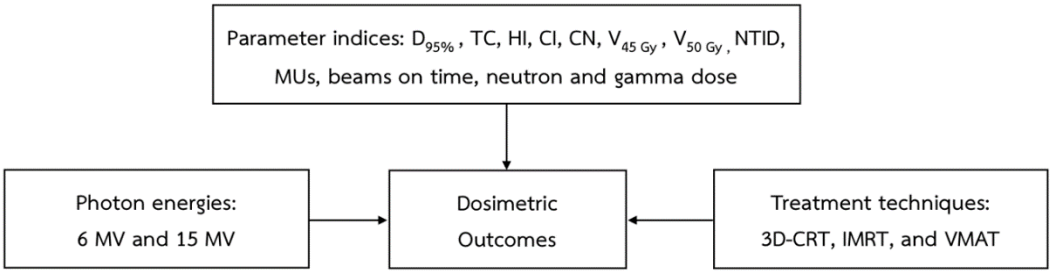

Figure 3.3 Conceptual frameworks.

3.4 Keywords

- Photon energy effect
- Cervical carcinoma
- 3D-CRT planning technique
- IMRT planning technique
- VMAT planning technique

3.5 Research question

What is the suitable photon energy between 6 MV and 15 MV photon beams in 3D-CRT, IMRT, and VMAT plans for cervical carcinoma?

3.6 Materials

The materials used in this study are from the Department of Radiation Oncology, King Chulalongkorn Memorial Hospital.

1) The advanced cervical cancer plans of 5 cases during 2016-2017 (figure 3.4), which have target volume in the range from 1,627.9 to 2,115.8 cm^3.

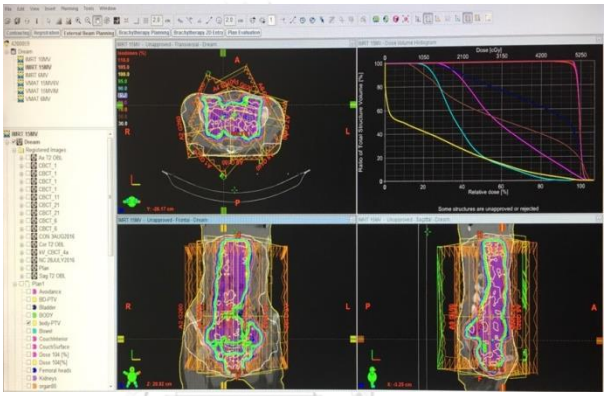

Figure 3.4 Dose distribution and DVHs of advanced cervical cancer plans.

2) Eclipse treatment planning system (TPS) with Anisotropic Analytical Algorithm. (version 11.0.31) (17)

The Analytical Anisotropic Algorithm (AAA) (Varian Medical System, Inc, Palo Alto, CA, USA) in Eclipse™ Integrated Treatment Planning was used in this study. This algorithm provides a fast and accurate dose calculation for clinical photon beams. The AAA dose calculation model is a 3D pencil beam convolution-superposition algorithm that separates modelling for primary photons, scattered extra-focal photons, and electrons scattered from the beam limiting devices. Functional forms for the fundamental physical expressions in AAA allows analytical convolution and thus reducing the computation time significantly.

3) Varian clinac 23EX linear accelerator

This study used Varian clinac 23EX linear accelerator with 120 millenium MLC (Varian Medical system, Inc, Palo Alto, USA), as shown in figure 3.5. The machine can be operated in 6 MV and 15 MV for photon beams and 4, 6, 9, 12, 16 and 20 MeV for electron beams. The range of field sizes are from 0.5x0.5 cm^2 to 40×40 cm^2 at isocenter. The distance from the target to isocenter is 100 cm. The dose rates can be adjusted from 100 to 600 MU/min for conventional mode. The 6 MV and 15 MV for photon beams were used in this study.

Figure 3.5 The Varian clinac 23EX linear accelerator.

4) Alderson rando phantom

The Alderson rando phantom (The Phantom laboratory, Salem, NY, USA) (figure 3.6) is molded of tissue-equivalent material which has the similar effective atomic number to the body's soft tissue. The material is radiologically equivalent to soft tissue and virtually indestructible, capable of withstanding substantial impact, and continuous handling without damage.

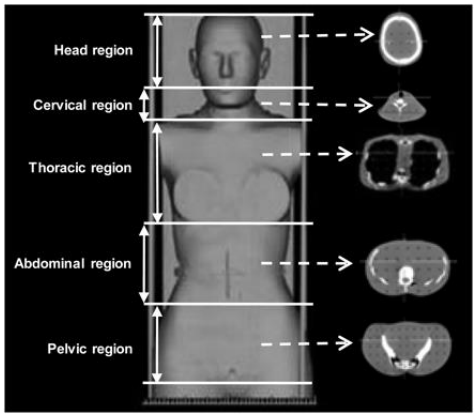

Figure 3.6 The Alderson rando phantom.

The materials used for neutron dosimetry are from the Department of Nuclear Engineering, Faculty of Engineering, Chulalongkorn University.

5) NE2 Neutron monitor (NE Technology)

Figure 3.7 shows the NE2 Neutron monitor (NE Technology, Limited, UK). It is the active neutron cylindrical polyethylene moderator that can decelerate fast neutrons into thermal neutrons and be detected by the central BF_3 tube. This detector possess good respond to thermal neutrons. The dose equivalent rate is expressed in terms of mSv/hr.

Figure 3.7 Anterior and lateral views of NE2 Neutron monitor.

6) HDS-101 GN Area survey meter (Mirion)

The HDS-101 GN Area survey meter (Mirion Technologies, Inc, Smyrna, Georgia, USA) as displayed in figure 3.8 has a high sensitivity and fast response active gamma-neutron detector. Three detectors are embedded in one probe. There are CsI (Tl) scintillator for low gamma dose rate measurement, Silicon diode for high gamma dose rate measurement, and LiI (Eu) scintillator for neutron measurement. The survey meter is able to detect gamma rays and neutrons in the range of 30 keV to 3 MeV and 0.025 eV to 15 MeV, respectively.

Figure 3.8 HDS-101 GN Area survey meter.

3.7 Methods

Part 1: Perform in planning room

1) Select the original advanced cervical plans which target and organs at risk were contoured by radiation oncologist.

2) Re-plan with 3D-CRT, IMRT and VMAT techniques on Eclipse TPS for 6 MV photon energy with the plan parameters as displayed in the figure 3.9.

<table>
<tr><td rowspan="2">Parameters</td><td colspan="3">Treatment techniques</td></tr>
<tr><td>3D-CRT</td><td>IMRT</td><td>VMAT</td></tr>
<tr><td>Number of fields / arcs</td><td>4 fields</td><td>9 fields</td><td>2 arcs</td></tr>
<tr><td>Photon energy</td><td colspan="2">6 MV</td><td>15 MV</td></tr>
<tr><td>Prescribed dose</td><td colspan="3">50.4 Gy in 28 fractions.</td></tr>
<tr><td>Tolerance dose limits</td><td colspan="3">
<table>
<tr><td rowspan="2">OARs</td><td rowspan="2">Dmax</td><td colspan="2">DVH</td></tr>
<tr><td>Dose</td><td>Max Volume</td></tr>
<tr><td>Bladder
Rectum</td><td>60</td><td>50 Gy</td><td>50%</td></tr>
<tr><td>Bowel</td><td>50</td><td>45 Gy</td><td>10%</td></tr>
</table>
</td></tr>
</table>

Figure 3.9 Treatment plan parameters in each technique and tolerance dose limits.

* In case of IMRT and VMAT plans the similar dose constraints was selected, while in case of 6 MV and 15 MV the similar optimization was performed.

3) Create the new plans by changing only the 6 MV photon to 15 MV photon plans. All other parameters remain constant.

4) Re-calculate the new plans.

5) Evaluate the plans using DVH and tolerance limit as shown in the figure 3.9.

6) Record the data from all treatment plans.

Part 2: Perform in treatment room

7) Open the treatment plans at the control room and transfer the plans to 23EX treatment room.

8) Set up the Alderson rando phantom on the couch (figure 3.10).

Figure 3.10 The Alderson rando phantom in AP head first position on the couch and the NE2 detectors at 1 m. in lateral and longitudinal far away from isocenter in the 23EX treatment room.

9) Place the NE2 detectors at diagram position from isocenter at 1 m. in lateral and longitudinal far away from isocenter in the treatment room (figure 3.10, 3.11, and 3.13). On the other hand, place the HDS-101 on console in control room (figure 3.12 and 3.13) to detect neutron during irradiation. The HDS-101 is placed toward the isocenter.

Figure 3.11 The NE2 detector at 1 m. in lateral and longitudinal direction far away from isocenter in the 23EX treatment room.

Figure 3.12 The HDS-101 on console in control room.

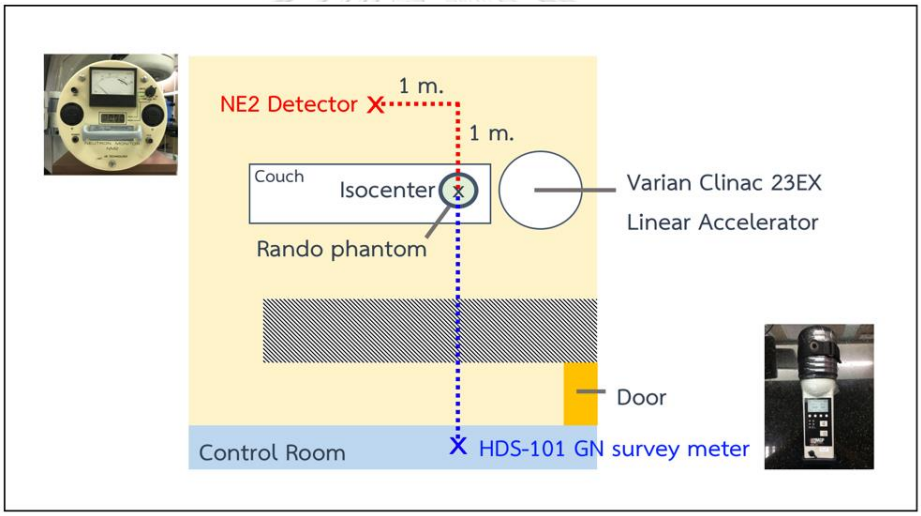

Figure 3.13 The 23EX treatment room diagram which illustrates the position of both detectors during irradiation.

10) Irradiate all 15 MV plans and observe the dose value on monitors.

11) Inside the treatment room, place the HDS-101 away from isocenter in diagram position of 1 m. lateral and longitudinal direction. Record neutron and gamma dose rate at 30s, 2mins, and 5mins after irradiation as displayed in figure 3.14.

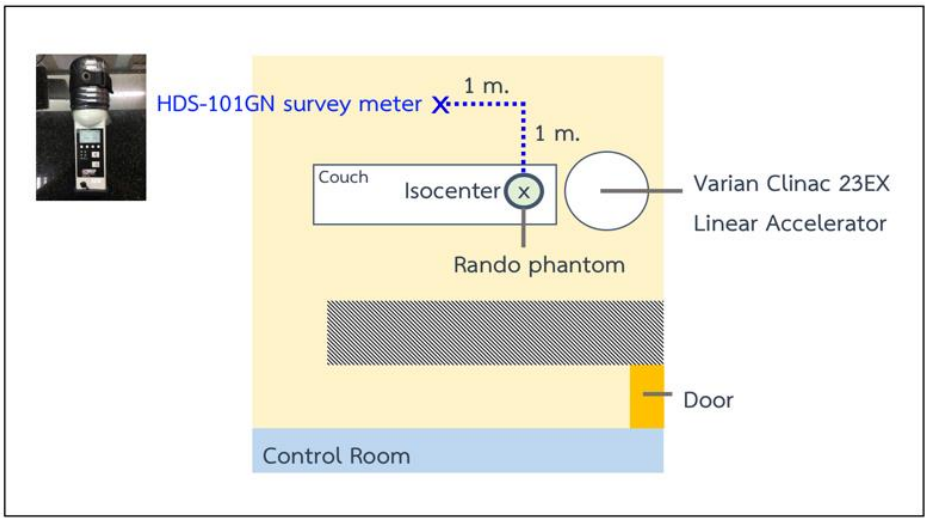

Figure 3.14 The 23EX treatment room diagram which shows position of HDS-101 GN detector after irradiation.

12) Analyze the results.

Evaluation parameters:

Record the data from treatment plans and dosimeters as shown in figure 3.15**.**

PTV	$D_{95\%}$, TC, HI, CI, and CN
OARs	Bladder, Rectum : $V_{50\ Gy}$ Bowel : $V_{45\ Gy}$
Parameter indices	NTID, MUs, and beam on time
Contamination dose	neutron and gamma dose

Figure 3.15 The recorded parameters for PTV, OARs, parameter indices, and contamination dose.

3.8 Outcome measurements

The outcomes for plan evaluation are:

- Dosimetric parameter of planning target volume (PTV)
- Dosimetric parameter of organs at risk (OARs)
- Target coverage (TC)
- Homogeneity index (HI)

- Conformity index (CI)
- Conformation number (CN)
- Normal tissue to integral dose (NTID)
- Total number of monitor units (MUs)
- Beam on time
- Neutron and Gamma dose

3.9 Statistical analysis

The mean and standard deviation of dosimetric parameters and neutron doses calculation were analyzed by using SPSS (Statistical Package for the Social Science for Windows) version 22 and Microsoft Excel version 2010.

3.10 Expected benefits

To obtain the information about the suitable energy in 3D-CRT, IMRT, and VMAT to treat patients with cervical cancer.

3.11 Ethical consideration

Although this study was performed in treatment planning system and in phantom, patient information was used. Therefore, the ethical consideration was submitted and has been approved by Ethics Committee of Faculty of Medicine, Chulalongkorn University. The number of approval is IRB No. 513/59 and the certificate is given in figure 3.16.

COE No. 017/2017
IRB No. 362/60

INSTITUTIONAL REVIEW BOARD
Faculty of Medicine, Chulalongkorn University
1873 Rama IV Road, Pathumwan, Bangkok 10330, Thailand. Tel 662-256-4493

Certificate of Exemption

The Institutional Review Board of the Faculty of Medicine, Chulalongkorn University, Bangkok, Thailand, has exempted the following study in compliance with the International guidelines for human research protection as Declaration of Helsinki, The Belmont Report, CIOMS Guideline, International Conference on Harmonization in Good Clinical Practice (ICH-GCP) and 45CFR 46.101(b)

Study Title : The dosimetric evaluation on photon energy effect for cervical cancer in 3D-CRT, IMRT and VMAT plans

Principal Investigator : Miss Vanida Poolnapol

Study Center : Department of Radiology, Faculty of Medicine, Chulalongkorn University

Signature: (Emeritus Professor Tada Suebkinyong MD) Chairperson, The Institutional Review Board

Signature: (Assistant Professor Prapapan Rajatapiti MD, PhD) Member and Secretary, The Institutional Review Board

Date of Exemption : July 5, 2017

Note No continuing review report and final report when finish require

Figure 3.16 The certificate of approval from ethic committee of Faculty of Medicine Chulalongkorn University.

CHAPTER IV

RESULTS

4.1 PTV

4.1.1 3D-CRT planning technique

The comparison of dosimetric parameters between 6 MV and 15 MV photon energies in 3D-CRT 4F-Box technique is shown in Table 4.1. (The raw data are shown in Table A1. and Table A2. of appendix). The PTV requires dose at least 50.4 Gy of prescription dose. For other parameters in both energies were not much different. Furthermore, the CI and CN from 15 MV presented better outcome than 6 MV since the mean was slightly closer to 1. This finding was supported by the data from p-value.

Table 4.1 The dosimetric parameters of PTV in 3D-CRT planning technique between 6 and 15 MV photon beams.

	6 MV	15 MV	P-value
$D_{95\%}$ (Gy)	50.624 ± 0.184	50.682 ± 0.166	0.228
TC (%)	96.694 ± 1.205	96.695 ± 0.974	0.998
HI	0.139 ± 0.044	0.113 ± 0.024	0.109
CI	0.551 ± 0.072	0.586 ± 0.088	0.024
CN	0.532 ± 0.063	0.566 ± 0.081	0.027

4.1.2 IMRT technique

The comparison of dosimetric parameters between 6 MV and 15 MV photon energies in IMRT technique is shown in Table 4.2. (The raw data are displayed in Table A3. and Table A4. of appendix). The PTV volume received doses nearly prescription dose in 50.4 Gy, while the other parameters of both energies were not much different.

Table 4.2 The dosimetric parameters of PTV in IMRT planning technique between 6 and 15 MV photon beams.

	6 MV	15 MV	P-value
$D_{95\%}$ (Gy)	50.643 ± 0.168	50.586 ± 0.184	0.550
TC (%)	96.657 ± 0.937	96.552 ± 0.759	0.661
HI	0.084 ± 0.003	0.074 ± 0.011	0.067
CI	0.890 ± 0.018	0.902 ± 0.023	0.050
CN	0.864 ± 0.023	0.871 ± 0.023	0.059

4.1.3 VMAT technique

The comparison of dosimetric parameters between 6 MV and 15 MV photon energies in VMAT technique is shown in Table 4.3. (The raw data are presented in Table A5. and Table A6. of appendix). The PTV volume obtained the prescription dose within 50.4 Gy. For other parameter indices, the outcome was similar to the IMRT technique.

Table 4.3 The dosimetric parameters of PTV in VMAT planning technique between 6 MV and 15 MV photon beams.

	6 MV	15 MV	P-value
$D_{95\%}$ (Gy)	50.480 ± 0.084	50.580 ± 0.148	0.298
TC (%)	96.072 ± 0.547	96.322 ± 0.336	0.485
HI	0.091 ± 0.017	0.095 ± 0.018	0.551
CI	0.915 ± 0.032	0.915 ± 0.043	0.980
CN	0.879 ± 0.035	0.881 ± 0.041	0.465

4.2 OARs

4.2.1 3D-CRT planning technique

Figure 4.1 exhibits the OARs dosimetric parameters comprised of $V_{50\ Gy}$ of bladder and rectum and $V_{45\ Gy}$ of bowel. The tolerance limit states that the volume of bladder and rectum obtaining dose 50 Gy should receive radiation dose below 50% of volume. For bowel volume receiving dose 45 Gy should receive radiation dose below 10% of volume. The 3D-CRT planning techniques displayed exceeding tolerance dose limits in both energies lead to the increased complications. (The raw data are shown in Table A1. and Table A2. of appendix)

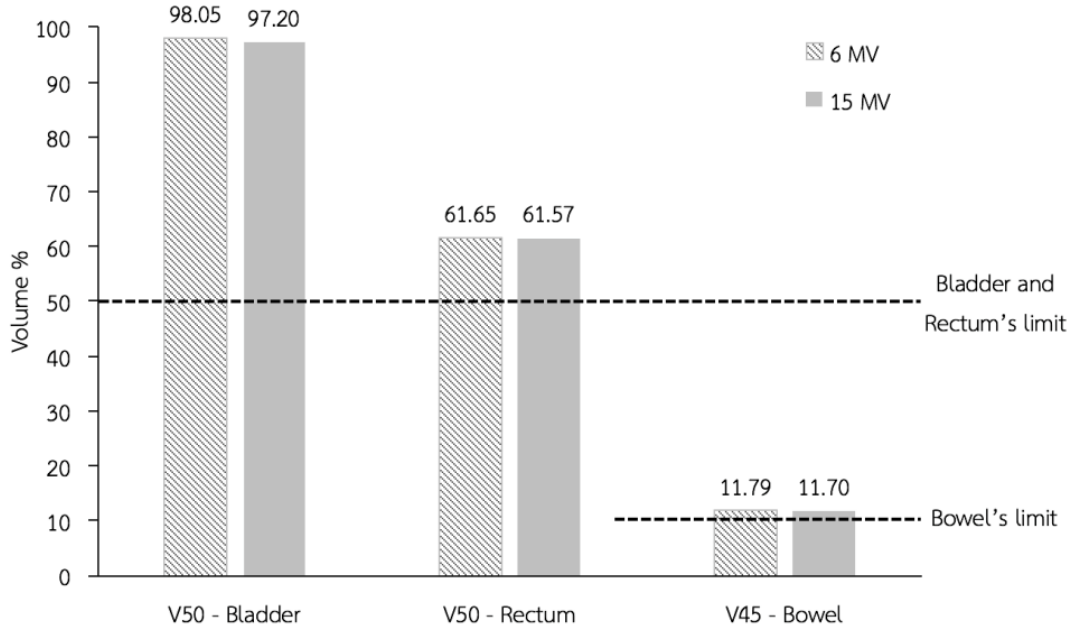

Figure 4.1 The dosimetric results of OARs in 3D-CRT planning technique between 6 and 15 MV photon beams.

4.2.2 IMRT planning technique

The dosimetric parameters of OARs comparison between 6 and 15 MV photon energies in IMRT technique is displayed in figure 4.2. The great similar doses between both photon energies were shown. For OARs, the outcomes were also still within tolerance limit. (The raw data are displayed in Table A3. and Table A4. of appendix).

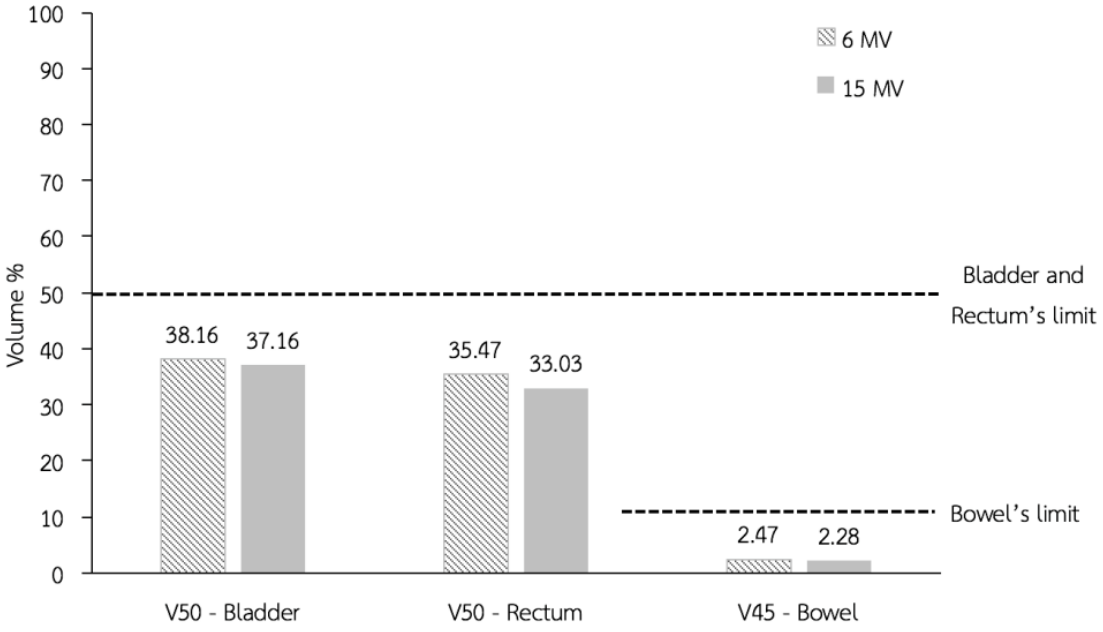

Figure 4.2 The dosimetric results of OARs in IMRT planning technique between 6 and 15 MV photon beams.

4.2.3 VMAT planning technique

The dosimetric parameters of OARs comparison between 6 MV and 15 MV photon energies in VMAT technique demonstrate the dose of all organs in both energy plans received similar dose and also within the tolerance limit for all OARs as displayed in figure 4.3. (The raw data are presented in Table A5. and Table A6. of appendix).

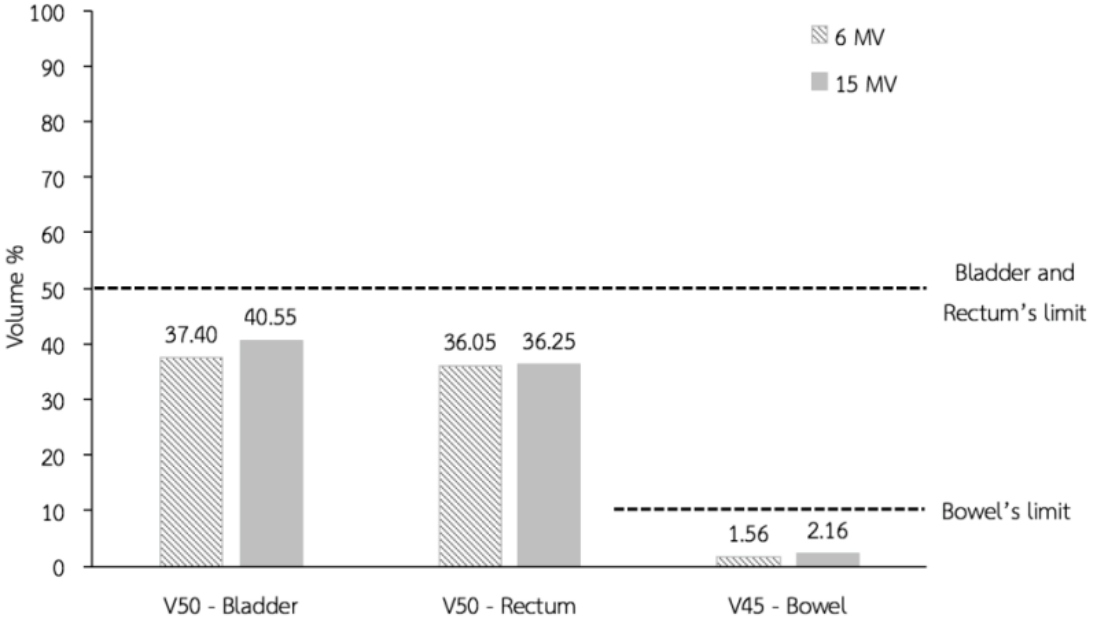

Figure 4.3 The dosimetric results of OARs in VMAT planning technique between 6 and 15 MV photon beams.

4.3 Parameter indices

4.3.1 3D-CRT planning technique

Table 4.4 lists the NTID, MUs and beam on time in 3D-CRT planning technique for both photon energies. The NTID from 15 MV was lower than 6 MV. In case of MU comparison, the 3D-CRT 4F-Box technique used lower MU in 15 MV. Therefore, the beam on time decreased in higher energy plans. (The raw data are shown in Table A1. and Table A2. of appendix)

Table 4.4 The dosimetric parameter indices in 3D-CRT planning technique between 6 and 15 MV photon beams.

	6 MV	15 MV	P-value
NTID (Gy.lit)	361.766 ± 127.787	335.842 ± 115.072	0.012
MUs	333.620 ± 23.036	279.120 ± 12.635	< 0.001
Beam on time (min)	0.834 ± 0.058	0.698 ± 0.032	< 0.001

4.3.2 IMRT planning technique

The dosimetric parameters comparison between 6 and 15 MV photon energies in IMRT planning technique is shown in Table 4.5. The NTID, MUs and beam on time were lower in higher energy plans. (The raw data are displayed in Table A3. and Table A4. of appendix).

Table 4.5 The dosimetric parameter indices in IMRT planning technique between 6 and 15 MV photon beams.

	6 MV	15 MV	P-value
NTID (Gy.lit)	338.818 ± 137.958	328.577 ± 125.693	0.148
MUs	2211.600 ± 374.638	1931.800 ± 236.468	0.024
Beam on time (min)	5.529 ± 0.938	4.830 ± 0.591	0.024

4.3.3 VMAT planning technique

The dosimetric parameter comparison between 6 MV and 15 MV photon energies in VMAT planning techniques is shown in table 4.6. All of parameter indices of 15 MV plans yielded the lower outcome than the 6 MV plans similar to the comparison in IMRT plans. (The raw data of NTID and MUs are shown in Table A5. and Table A6. While, the raw data of beam on time are shown in Table A7. of appendix)

Table 4.6 The dosimetric parameter indices in VMAT planning technique between 6 and 15 MV photon beams.

	6 MV	15 MV	P-value
NTID (Gy.lit)	323.984 ± 130.064	310.821 ± 123.779	0.012
MUs	448.600 ± 36.814	405.600 ± 50.317	0.015
Beam on time (min)	1.267 ± 0.007	1.215 ± 0.001	0.478

4.4 Neutron and Gamma dose

4.4.1 During irradiation

Figure 4.4 and 4.5 (The raw data are demonstrated in Table A8.) show the neutron dose rate in all treatment techniques during treatment. The NE2 neutron monitor was placed inside treatment room while the HDS-101GN area survey meter was positioned outside the treatment room. Inside the treatment room, the Alderson Rando phantom was irradiated using 15 MV photon beams. The neutron product from IMRT planning technique exhibited the highest number of neutron dose rate compared to 3D-CRT and VMAT, respectively.

4.4.2 After irradiation

Figure 4.6 and 4.7 show neutron and gamma dose in all treatment techniques at 30s, 2mins, and 5mins after treatment. The HDS-101 GN area survey meter was placed inside the treatment room and Alderson rando phantom was irradiated using 15 MV photon beams. The IMRT planning technique produced higher number of neutron and gamma dose rate than VMAT and 3D-CRT, respectively. (The raw data are presented in Table 9A., Table 10A., and Table 11A.)

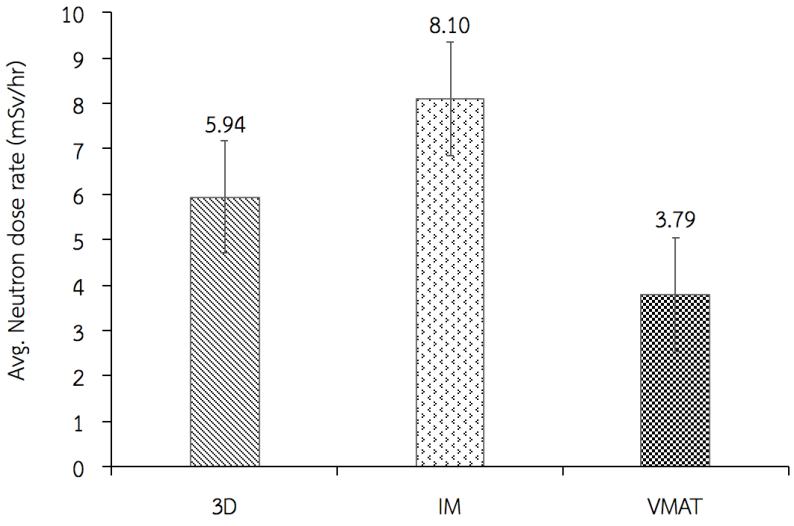

Figure 4.4 Comparison of neutron dose rate (mSv/hr) measured by NE2 detector at 1 m. far away from isocenter during treatment from 3D-CRT, IMRT, and VMAT planning techniques.

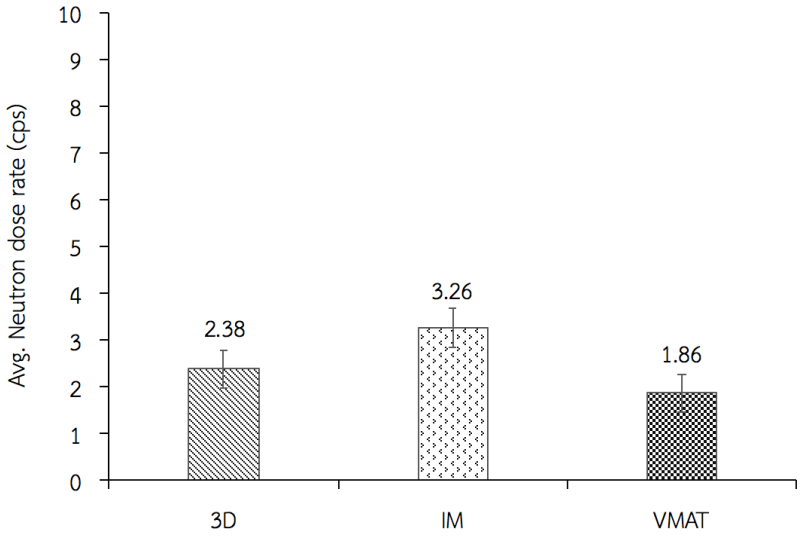

Figure 4.5 Comparison of neutron dose rate (cps) measured by HDS-101 GN area survey meter at control room during treatment from 3D-CRT, IMRT, and VMAT planning techniques.

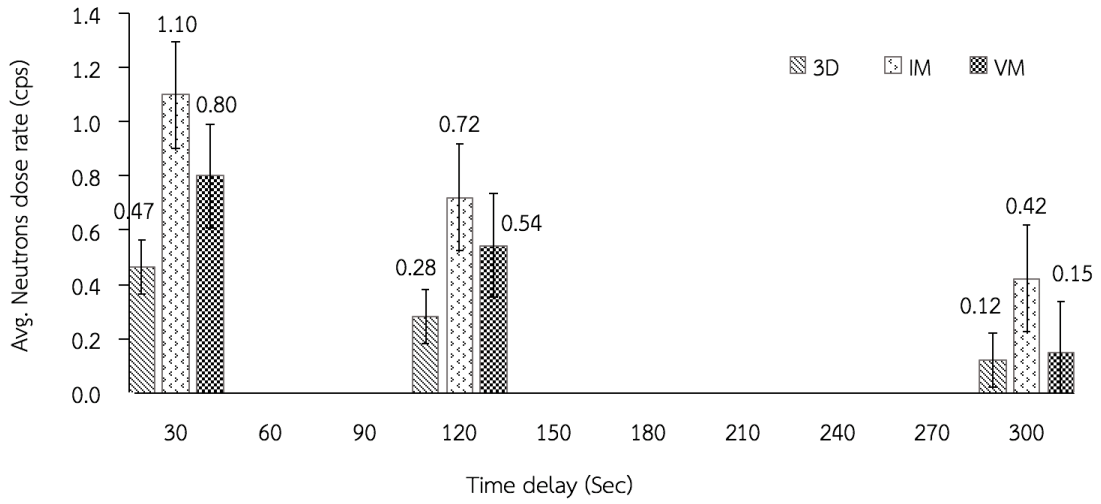

Figure 4.6 Comparison of neutron dose rate (cps) at 30s, 2mins, and 5mins measured by HDS-101 GN area survey meter at 1 m. far away from isocenter after treatment from 3D-CRT, IMRT, and VMAT planning techniques.

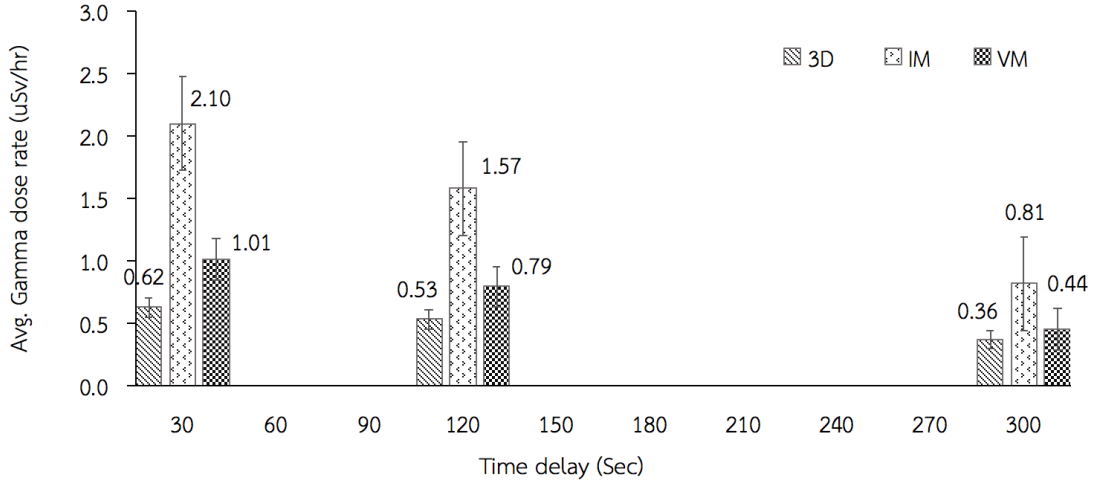

Figure 4.7 Comparison of gamma dose rate (uSv/h) at 30s, 2mins, and 5mins measured by HDS-101 GN area survey meter at 1 m. far away from isocenter after treatment from 3D-CRT, IMRT, and VMAT planning techniques.

CHAPTER V

DISCUSSION AND CONCLUSION

5.1 DISCUSSION

According to the results, it was clear that both energies had the advantages as well as the drawbacks which could affect the decision to select the suitable energy in each technique. We noticed that the higher energy was the good alternative of 3D-CRT 4 fields box technique in large patient due to the higher penetration to the target. In contrast, the lower energy of 3D-CRT plans was unable to transfer the similar dose to the tumor, in which the same isodose line was selected to evaluate the 4 fields box technique. This reason was expressed in forms of CI and CN indices. The CI of higher energy provided value of 0.586 ± 0.088 that was better than lower energy of 0.551 ± 0.072. The CN of 15 MV provided value of 0.566 ± 0.081 that was better than 6 MV of 0.532 ± 0.063 with statistically significant difference as supported from the table 4.1. Furthermore, the OARs of 6 MV plans received slightly more radiation dose than the OARs of 15 MV plans (Figure 4.1) due to the lower penetration power of lower energy including the pelvis thickness. Besides, the higher energy beams also showed the better outcomes in terms of NTID, MUs, and beam on time for all techniques. The 3D-CRT displayed exceeding tolerance dose limits in both energies which potentially lead into the high complication rates. There are both acute and long-term potential complications that tend to start a few days after the beginning of radiotherapy. These symptoms include diarrhea, bladder inflammation, bleeding from the vagina, tiredness, and weakness. Late effects could be the changes of the ovaries, the changes of the vagina, swelling, bladder effects, bowel effects, and bleeding. The side effects could continue or might start several months or years after treatment.

According to table 4.4, 4.5, and 4.6, the 15 MV photon energy showed the dose reduction of NTID, MUs, and beam on time for all planning techniques. The reduction of total number of monitor unit in 15 MV was caused by high penetration property of high energy. When the high energy was employed, the NTID decreased due to the less absorption of 15 MV in treated volume. Our results agreed to the Tyagi study (8). They observed the small differences between 6 MV and 15 MV for HI in IMRT plans for cervical cancer treatment and discovered that two energy plans were nearly identical in their conformity of dose to the target.

In this study, neutron doses in 6 MV photon energy of all planning techniques were not measured, since the 10 MV photon is the border energy to induce the neutron production. In addition, study from F. KRY et al. (12) found that no neutron contribution in 6 MV and only minimal neutron contribution was detected at 10 MV (typically 1%) of IMRT technique in both of Varian and Siemens linear accelerators.

In our research, during the beam irradiation to phantom, the neutron contamination from IMRT was much higher compared to the 3D-CRT and VMAT technique. This finding was corresponded to the higher MUs from IMRT in comparison to other techniques. However, the neutron contamination from 3D-CRT was higher than VMAT even though the MUs from VMAT was

relatively higher than 3D-CRT. In 3D-CRT, 4 fields box technique was employed and hence the gantry rotated within four different angles. The radiation toward the NE2 neutron detector varied across the gantry rotation. Therefore, the beam angle dependence was more pronounced and affected the measured dose from this detector. The reading became significantly higher when the gantry rotation was 270 degrees and lower when the gantry rotated to 90 degrees. In part of HDS-101 GN area survey meter which placed on the control room, the 90 degree gantry rotation was significantly higher than gantry rotated to 270 degree.

After the beam irradiation, the neutron contamination from IMRT was still higher than other techniques. However, the trend changed as we found the VMAT technique produced higher neutron contamination than 3D-CRT. Once the beam irradiation was completed, the measurements were made after 30s, 2mins, and 5mins. During that period, the neutron has spread around the treatment room and the gantry direction still in the 0 degree position. Therefore, neutron doses collected by using HDS-101 GN area survey meter (placed inside treatment room) from 3D-CRT became lower than VMAT technique.

For gamma doses, we observed the result only after irradiation. The results showed the same trend as neutron doses collected by using HDS-101 GN area survey meter place in side treatment room at 1 m. far way form isocenter. The gamma contamination generated by IMRT after treatment of 30s, 2mins, and 5mins was higher approximately one time to VMAT and two times to 3D-CRT plans.

Therefore, the neutron and gamma contamination in the head of linear accelerator from higher energy of IMRT plans were more pronounced than other techniques. Our study agreed well to study from F. Vanhavere et al. (16) where they illustrated neutron and gamma peripheral doses around a medical accelerator in 6 MV and 18 MV photon energies of IMRT techniques were higher for 18 MV compared with 6 MV photon beams. For 6 MV photon beam, both neutron and gamma dose could be neglected.

5.2 CONCLUSION

For 3D-CRT technique, 15 MV photon beams is recommended to yield more uniform dose distribution in cervical cancer region with small amount of neutron and gamma doses. On the other hand, for IMRT planning technique, the 6 MV photon beams is a suitable option for cervical carcinoma treatment as this energy produced similar outcome to 15 MV photon beams and possess no neutron and gamma contamination. For VMAT planning technique, both of the photon energies could be selected to treat cervical cancer. There is no significant different between these two energies in dosimetric parameters as well as the contamination dose since 15 MV photon beams produced a small amount of neutron and gamma contamination.

REFERENCES

1. Ferlay J, Soerjomataram I, Dikshit R, Eser S, Mathers C, Rebelo M, et al. Cancer incidence and mortality worldwide: sources, methods and major patterns in GLOBOCAN 2012. Int J Cancer. 2015;136(5):E359-86.
2. L. PORTELANCE. INTENSITY-MODULATED RADIATION THERAPY (IMRT) REDUCES SMALL BOWEL, RECTUM, AND BLADDER DOSES IN PATIENTS WITH CERVICAL CANCER RECEIVING PELVIC AND PARA-AORTIC IRRADIATION. Radiation Oncology Biol Phys. 2001;51:261-6.
3. Deng X, Han C, Chen S, Xie C, Yi J, Zhou Y, et al. Dosimetric benefits of intensity-modulated radiotherapy and volumetric-modulated arc therapy in the treatment of postoperative cervical cancer patients. J Appl Clin Med Phys. 2017;18(1):25-31.
4. Phoolcharoen N, Kantathavorn N, Sricharunrat T, Saeloo S, Krongthong W. A population-based study of cervical cytology findings and human papillomavirus infection in a suburban area of Thailand. Gynecol Oncol Rep. 2017;21:73-7.
5. Soiety AC. Cervical Cancer [16122017]. Available from: https://www.cancer.org/cancer/cervical-cancer/causes-risks-prevention/what-causes.html
6. E.B. P. Radiation Oncology Physics A Handbook for Teachers and Students. . International Atomic Energy Agency Wagramer Strasse 5, P.O. Box 100, A-1400 Vienna, 2005.
7. Lomax NJ, Scheib SG. Quantifying the degree of conformity in radiosurgery treatment planning. International Journal of Radiation Oncology*Biology*Physics. 2003;55(5):1409-19.
8. Tyagi A, Supe SS, Sandeep, Singh MP. A dosimetric analysis of 6 MV versus 15 MV photon energy plans for intensity modulated radiation therapy (IMRT) of carcinoma of cervix. Rep Pract Oncol Radiother. 2010;15(5):125-31.
9. Khan F GJ. The Physics of Radiation Therapy. 5th Edition. Two Commerce Square 2001 Market Street Philadelphia, PA 19103 USA2014.
10. ไพศาลกิตติสกลุ น. ฟิสิกส์เชิงรังสี (Radiological Physics). 2555. . กรุงเทพมหานคร p.
11. Awotwi-Pratt JB, Spyrou NM. Measurement of photoneutrons in the output of 15 MV varian clinac 2100C LINAC using bubble detectors. Journal of Radioanalytical and Nuclear Chemistry. 2007;271(3):679-84.
12. Kry et al SFK, Bryan Bednarz, Rebecca M. Howell and Larry Dauer. AAPM TG 158: Measurement and calculation of doses outside the treated volume from external-beam radiation therapy. 2017 American Association of Physicists in Medicine. 2017:e406.
13. J. W. Scintillation Detector 2006 [cited 2017 12,Dec]. Available from: https://www.cefns.nau.edu/geology/malabs/Microprobe/WDS-Scintillation.html

14. RADIATION DETECTOR [Available from: https://www.britannica.com/science/solid-state-detector.
15. Forrest J, Presutti J, Davidson M, Hamilton P, Kiss A, Thomas G. A dosimetric planning study comparing intensity-modulated radiotherapy with four-field conformal pelvic radiotherapy for the definitive treatment of cervical carcinoma. Clin Oncol (R Coll Radiol). 2012;24(4):e63-70.
16. Vanhavere F, Huyskens D, Struelens L. Peripheral neutron and gamma doses in radiotherapy with an 18 MV linear accelerator. Radiat Prot Dosimetry. 2004;110(1-4):607-12.
17. Sievinen J UW, Kaissl K. . AAA Photon Dose Calculation Model in EclipseTM.:1.-23.

Table A1. The dosimetric data of 6 MV 3D-CRT plans.

6 MV																							
Pt. No.	DOSE (Gy)								V_{50Gy} (%)		V_{45Gy} (%)	PTV Volume (cm^3)			Body-PTV		TC	CI	HI	CN	NTID	MUs	Beams on time
	PTV					mean dose of OAR																	
	$D_{98\%}$	$D_{95\%}$	$D_{50\%}$	$D_{2\%}$	Mean Dose	BD	RT	B	BD	RT	B	V_t	V_{pi}	$V_{t,pi}$	Vol. (lit)	mean dose (Gy)							
1	50.2	50.6	53.3	55.8	53.3	52.8	44.1	31.5	100.0	42.9	19.6	1627.9	3354.6	1599.2	31.1	11.3	98.24	0.48	0.11	0.47	351.9	331.1	0.83
2	50.1	50.8	53.5	55.7	53.4	51.3	46.3	33.2	100.0	53.0	21.6	1421.9	2680.3	1387.9	7.4	27.6	97.61	0.52	0.10	0.51	203.1	299.1	0.75
3	49.7	50.8	54.8	59.4	54.6	55.4	57.8	26.2	100.0	99.7	7.2	2413.5	4612.5	2328.7	39.9	13.7	96.49	0.50	0.18	0.49	546.6	358.1	0.90
4	49.4	50.4	54.4	55.7	53.9	53.4	52.6	27.9	97.9	97.2	3.3	1860.0	2882.8	1779.3	36.0	11.3	95.66	0.62	0.12	0.59	407.1	351.0	0.88
5	49.0	50.5	55.8	59.9	55.5	51.7	44.7	35.5	92.4	15.4	7.2	2115.8	3169.7	2020.1	20.6	14.6	95.48	0.64	0.19	0.61	300.1	328.8	0.82
Avg.	49.7	50.6	54.4	57.3	54.2	52.9	49.1	30.8	98.0	61.7	11.8	1887.8	3340.0	1823.0	27.0	15.7	96.69	0.55	0.14	0.53	361.8	333.6	0.83
SD	0.5	0.2	1.0	2.2	0.9	1.6	5.9	3.8	3.3	36.3	8.2	391.7	757.1	366.0	13.2	6.8	1.21	0.07	0.04	0.06	127.8	23.0	0.06

Table A2. The dosimetric data of 15 MV 3D-CRT plans.

15 MV																							
Pt. No.	DOSE (Gy)								V_{50Gy} (%)		V_{45Gy} (%)	PTV Volume (cm^3)			Body-PTV		TC	CI	HI	CN	NTID	MUs	Beams on time
	PTV					mean dose of OAR																	
	$D_{98\%}$	$D_{95\%}$	$D_{50\%}$	$D_{2\%}$	Mean Dose	BD	RT	B	BD	RT	B	V_t	V_{pi}	$V_{t,pi}$	Vol. (lit)	mean dose (Gy)							
1	49.8	50.7	52.7	54.7	52.7	52.3	42.4	30.6	100.0	40.3	18.9	1627.9	3125.7	1574.3	31.1	10.6	96.71	0.50	0.09	0.49	330.1	278.2	0.70
2	49.4	50.8	53.5	55.6	53.4	52.3	46.5	32.5	100.0	59.6	23.5	1421.9	2665.4	1389.0	7.4	26.5	97.69	0.52	0.12	0.51	195.0	260.7	0.65
3	49.9	50.8	53.5	57.3	53.7	55.0	54.1	25.4	100.0	100.0	7.2	2413.5	4340.47	2347.9	39.9	12.6	97.28	0.54	0.14	0.53	504.3	293.9	0.73
4	49.5	50.4	52.9	53.9	52.6	52.1	51.2	26.1	95.6	81.1	2.7	1860.0	2601.9	1769.3	36.0	10.3	95.12	0.68	0.08	0.65	372.2	287.3	0.72
5	49.9	50.7	54.6	57.1	54.4	51.2	44.9	32.7	90.4	26.8	6.1	2115.8	2997.8	2045.5	20.6	13.5	96.68	0.68	0.13	0.66	277.6	275.5	0.69
Avg.	49.7	50.7	53.4	55.7	53.3	52.6	47.8	29.5	97.2	61.6	11.7	1887.8	3146.3	1825.2	27.0	14.7	96.70	0.59	0.11	0.57	335.8	279.1	0.70
SD	0.2	0.2	0.7	1.5	0.7	1.4	4.8	3.5	4.3	29.7	9.0	391.7	702.9	380.2	13.2	6.7	0.97	0.09	0.02	0.08	115.1	12.6	0.03

Table A3. The dosimetric data of 6 MV IMRT plans.

6 MV																							
Pt. No.	DOSE (Gy)								V_{50Gy} (%)		V_{45Gy} (%)	PTV Volume (cm^3)			Body-PTV		TC	CI	HI	CN	NTID	MUs	Beams on time
	PTV					mean dose of OAR																	
	$D_{98\%}$	$D_{95\%}$	$D_{50\%}$	$D_{2\%}$	Mean Dose	BD	RT	B	BD	RT	B	V_t	V_{pi}	$V_{t,pi}$	Vol. (lit)	mean dose (Gy)							
1	50.1	50.8	52.8	54.6	54.6	38.5	32.2	29.0	14.5	4.3	0.5	1627.9	1807.2	1586.6	31.1	10.5	97.46	0.88	0.09	0.86	327.6	2798.0	7.00
2	50.2	50.8	52.5	54.5	54.2	42.1	39.4	26.1	42.7	48.2	7.9	1421.9	1536.5	1391.0	7.4	23.6	97.83	0.91	0.08	0.89	173.4	2341.0	5.85
3	49.5	50.5	52.6	54.0	52.5	44.0	45.2	26.1	35.6	30.3	3.6	2413.5	2660.2	2310.1	39.9	13.5	95.72	0.87	0.09	0.83	539.0	1935.0	4.84
4	49.4	50.4	52.3	53.8	52.2	42.5	44.4	25.7	48.5	48.1	0.0	1860.0	1958.6	1784.7	36.3	10.8	95.95	0.91	0.09	0.87	391.3	1874.0	4.69
5	49.9	50.7	52.4	54.0	52.4	43.7	40.3	18.3	49.5	46.5	0.5	2115.8	2295.0	2038.1	20.6	12.8	96.33	0.89	0.08	0.86	262.8	2110.0	5.28
Avg.	49.8	50.6	52.5	54.2	53.2	42.2	40.3	25.1	38.2	35.5	2.5	1887.8	2051.5	1822.1	27.1	14.2	96.66	0.89	0.08	0.86	338.8	2211.6	5.53
SD	0.4	0.2	0.2	0.3	1.1	2.2	5.2	4.0	14.3	19.0	3.3	391.7	436.8	363.1	13.2	5.4	0.94	0.02	0.00	0.02	138.0	374.6	0.94

Table A4. The dosimetric data of 15 MV IMRT plans.

15 MV																							
Pt. No.	DOSE (Gy)								V_{50Gy} (%)		V_{45Gy} (%)	PTV Volume (cm^3)			Body-PTV		TC	CI	HI	CN	NTID	MUs	Beams on time
	PTV					mean dose of OAR																	
	$D_{98\%}$	$D_{95\%}$	$D_{50\%}$	$D_{2\%}$	Mean Dose	BD	RT	B	BD	RT	B	V_t	V_{pi}	$V_{t,pi}$	Vol. (lit)	mean dose (Gy)							
1	49.9	50.6	52.1	53.7	52.1	39.4	33.7	29.0	14.5	5.1	0.2	1627.9	1746.1	1577.7	31.1	10.3	96.92	0.90	0.07	0.88	320.4	2287.0	5.72
2	50.2	50.8	52.0	53.8	52.2	42.8	39.2	27.1	42.8	47.0	6.9	1421.9	1529.6	1388.5	7.4	23.8	97.65	0.91	0.07	0.89	175.2	2037.0	5.09
3	49.8	50.7	52.7	53.8	52.5	44.0	45.2	25.9	36.1	31.5	3.3	2413.5	2667.2	2318.4	39.9	12.8	96.06	0.87	0.08	0.83	511.5	1879.0	4.70
4	49.2	50.4	52.3	53.9	52.2	43.9	42.7	23.4	46.4	48.2	0.0	1860.0	1931.8	1793.4	36.0	10.3	96.42	0.93	0.09	0.90	372.2	1711.0	4.28
5	49.8	50.4	51.8	52.9	53.1	43.3	38.6	26.6	46.1	33.5	1.0	2115.8	2243.3	2025.1	20.6	12.8	95.71	0.90	0.06	0.86	263.6	1745.0	4.36
Avg.	49.8	50.6	52.2	53.6	52.4	42.7	39.9	26.4	37.2	33.0	2.3	1887.8	2023.6	1820.6	27.0	14.0	96.55	0.90	0.07	0.86	328.6	1931.8	4.83
SD	0.37	0.18	0.32	0.42	0.39	1.91	4.38	2.02	13.33	17.39	2.90	391.70	444.96	366.09	13.16	5.61	0.76	0.02	0.01	0.02	125.7	236.5	0.59

Table A5. The dosimetric data of 6 MV VMAT plans.

6 MV																						
Pt. No.	DOSE (Gy)								V_{50Gy} (%)		V_{45Gy} (%)	PTV Volume (cm^3)			Body-PTV		TC	CI	HI	CN	NTID	MUs
	PTV					mean dose of OAR																
	$D_{98\%}$	$D_{95\%}$	$D_{50\%}$	$D_{2\%}$	Mean Dose	BD	RT	B	BD	RT	B	V_t	V_{pi}	$V_{t,pi}$	Vol. (lit)	mean dose (Gy)						
1	49.8	50.5	53.1	54.7	52.9	38.1	36.2	27.0	6.1	3.5	0.6	1627.9	1709.8	1564.6	31.1	9.8	96.11	0.92	0.09	0.88	303.9	510.0
2	50.0	50.4	52.6	54.0	52.5	48.8	45.5	26.6	46.2	53.3	2.4	1421.9	1459.8	1367.2	7.4	22.7	96.15	0.94	0.08	0.90	168.0	448.0
3	49.4	50.4	53.9	55.8	53.5	45.4	47.3	24.3	37.7	35.1	4.4	2413.5	2668.2	2295.7	39.9	12.8	95.12	0.86	0.12	0.82	510.7	445.0
4	50.0	50.6	53.1	54.6	53.0	45.3	48.2	24.1	47.7	56.8	0.0	1860.0	1939.4	1797.7	36.0	10.6	96.65	0.93	0.09	0.90	381.9	419.0
5	49.8	50.5	52.4	53.9	53.3	45.8	38.6	23.9	49.3	31.6	0.4	2115.8	2177.3	2038.1	20.6	12.4	96.33	0.94	0.08	0.90	255.4	421.0
Avg.	49.8	50.5	53.0	54.6	53.0	44.7	43.2	25.2	37.4	36.0	1.6	1887.8	1990.9	1812.7	27.0	13.7	96.07	0.92	0.09	0.88	324.0	448.6
SD	0.2	0.1	0.6	0.8	0.4	3.9	5.4	1.5	18.1	21.3	1.8	391.7	462.9	368.9	13.1	5.2	0.57	0.03	0.02	0.04	130.1	36.8

Table A6. The dosimetric data of 15 MV VMAT plans.

15 MV																						
Pt. No.	DOSE (Gy)								V_{50Gy} (%)		V_{45Gy} (%)	PTV Volume (cm^3)			Body-PTV		TC	CI	HI	CN	NTID	MUs
	PTV					mean dose of OAR																
	$D_{98\%}$	$D_{95\%}$	$D_{50\%}$	$D_{2\%}$	Mean Dose	BD	RT	B	BD	RT	B	V_t	V_{pi}	$V_{t,pi}$	Vol. (lit)	mean dose (Gy)						
1	49.7	50.6	53.2	54.7	54.2	37.1	34.0	26.4	7.2	3.4	0.8	1627.9	1714.9	1572.2	31.1	9.4	96.58	0.92	0.09	0.89	293.3	472.0
2	50.0	50.5	53.6	54.1	52.5	48.7	45.0	26.4	56.9	48.4	5.6	1421.9	1461.4	1371.5	7.4	22.2	96.46	0.94	0.08	0.91	163.7	443.0
3	49.6	50.8	54.5	56.4	54.2	46.1	47.8	23.5	42.8	42.8	4.1	2413.5	2769	2327.2	39.9	12.3	96.42	0.84	0.12	0.81	490.8	391.0
4	49.7	50.6	53.2	54.6	53.0	45.5	48.3	23.3	48.0	56.2	0.0	1860.0	1913.8	1793.4	36.0	10.0	96.42	0.94	0.09	0.90	361.6	353.0
5	49.5	50.4	52.5	54.0	52.4	46.0	38.6	22.7	47.9	30.5	0.3	2115.8	2148.1	2025.5	20.6	11.9	95.73	0.94	0.09	0.90	244.6	369.0
Avg.	49.7	50.6	53.4	54.8	53.2	44.7	42.7	24.5	40.6	36.3	2.2	1887.8	2001.4	1818.0	27.0	13.2	96.32	0.92	0.09	0.88	310.8	405.6
SD	0.4	0.2	0.3	0.4	0.4	1.9	4.4	2.0	13.3	17.4	2.9	391.7	498.0	375.1	13.2	5.2	0.34	0.04	0.02	0.04	123.8	50.3

Table A7. The data for beam on time calculation in both energies of VMAT technique.

Pt. No.	Arc No.	6 MV				15 MV			
		Avg. Dose Rate [MU/min]	MU	Beams on time [min.]	Avg. Beams on time [min.]	Avg. Dose Rate [MU/min]	MU	Beams on time [min.]	Avg. Beams on time [min.]
1	1	210.89	256	1.21	1.21	189.64	230	1.21	1.22
	2	209.24	254	1.21		198.75	242	1.22	
2	1	177.99	216	1.21	1.21	167.81	204	1.22	1.21
	2	191.08	232	1.21		196.85	239	1.21	
3	1	210.89	262	1.24	1.23	185.08	225	1.22	1.21
	2	220.53	268	1.22		189.03	229	1.21	
4	1	167.44	203	1.21	1.21	148.70	181	1.22	1.22
	2	178.10	216	1.21		141.63	172	1.21	
5	1	157.73	192	1.22	1.22	134.54	163	1.21	1.21
	2	188.23	229	1.22		169.46	206	1.22	

Table A8. The data of neutron doses during irradiation in all 15 MV planning techniques.

Pt.No.	NM2 Neutron Dose rate (mSv/hr)			HDS-101 Neutron Dose rate (cps)		
	3D-CRT	IMRT	VMAT	3D-CRT	IMRT	VMAT
1	4.4	8.4	6.1	2.1	2.8	2.3
2	6.9	8.3	5.9	1.7	3.0	2.0
3	5.3	6.6	1.1	2.5	3.9	2.3
4	6.8	8.8	3.3	3.0	2.8	1.6
5	6.3	8.4	2.6	2.6	3.8	1.1
Avg	5.9	8.1	3.8	2.4	3.3	1.9
SD	1.1	0.8	2.2	0.5	0.5	0.5

Table A9. The data of neutron and gamma dose during and after irradiation by using HDS-101 GN area survey meter in 3D-CRT techniques.

Pt.No.	15 MV							
	Gamma (uS/h)				Neutrons (cps)			
	During irradiate	30s pass	2min. Pass	5min. Pass	During irradiate	30s pass	2min. Pass	5min. Pass
1	0.1	0.7	0.5	0.3	2.1	0.9	0.5	0.2
2	0.1	0.1	0.2	0.4	1.7	0.7	0.5	0.3
3	0.1	0.7	0.6	0.4	2.5	0.2	0.0	0.0
4	0.1	0.8	0.7	0.4	3.0	0.3	0.2	0.0
5	0.1	0.8	0.7	0.5	2.6	0.2	0.2	0.1
Avg	0.1	0.6	0.5	0.4	2.4	0.5	0.3	0.1
SD	0.0	0.3	0.2	0.1	0.5	0.3	0.2	0.1

Table A10. The data of neutron and gamma dose during and after irradiation by using HDS-101 GN area survey meter in IMRT techniques.

Pt.No.	15 MV							
	Gamma (uS/h)				Neutrons (cps)			
	During irradiate	30s pass	2min. Pass	5min. Pass	During irradiate	30s pass	2min. Pass	5min. Pass
1	0.1	3.0	1.9	0.9	2.8	0.7	0.1	0.3
2	0.1	0.5	1.1	0.9	3.0	2.5	1.8	0.5
3	0.1	2.2	1.2	0.4	3.9	0.9	0.7	0.9
4	0.1	2.3	1.6	0.9	2.8	0.8	0.7	0.4
5	0.1	2.5	2.0	1.0	3.8	0.6	0.3	0.0
Avg	0.1	2.1	1.6	0.8	3.3	1.1	0.7	0.4
SD	0.0	0.9	0.4	0.2	0.5	0.8	0.7	0.3

Table A11. The data of neutron and gamma dose during and after irradiation by using HDS-101 GN area survey meter in VMAT techniques.

Pt.No.	15 MV							
	Gamma (uS/h)				Neutrons (cps)			
	During irradiate	30s pass	2min. Pass	5min. Pass	During irradiate	30s pass	2min. Pass	5min. Pass
1	0.1	1.4	0.8	0.5	2.3	0.6	0.3	0.2
2	0.1	0.3	0.2	0.1	2.0	1.4	1.0	0..52
3	0.1	1.7	1.0	0.6	2.3	0.4	0.2	0.0
4	0.1	0.4	0.9	0.5	1.6	1.2	1.0	0.2
5	0.1	1.3	1.1	0.6	1.1	0.4	0.2	0.2
Avg	0.1	1.0	0.8	0.4	1.9	0.8	0.5	0.2
SD	0.0	0.6	0.3	0.2	0.5	0.5	0.4	0.1

VITA

Miss Vanida Poolnapol was born in Chonburi, Thailand on June 2, 1993. She graduated high school from Chonkanyanukoon School, Chonburi in 2011. She completed Bachelor's Degree of Science in Radiological Technology Program from Mahidol University in 2016. She continued to study Master's Degree of Science in Medical Imaging Program from Chulalongkorn University, Thailand since August 2016.